





DUDLEY KNOX LIBRARY  
NAVAL POSTGRADUATE SCHOOL  
MONTEREY CA 93943-5101





# NAVAL POSTGRADUATE SCHOOL

## Monterey, California



## THESIS

INVESTIGATIONS OF A SINGLE POINT  
TEMPERATURE PROBE FOR MEASUREMENT  
OF ATMOSPHERIC TURBULENCE

by

Cloyes R. Hoover

December, 1991

Thesis Advisor:

D. L. Walters

Approved for public release; distribution is unlimited.



unclassified

SECURITY CLASSIFICATION OF THIS PAGE

## REPORT DOCUMENTATION PAGE

Form Approved  
OMB No. 0704-0188

1a REPORT SECURITY CLASSIFICATION unclassified			1b RESTRICTIVE MARKINGS	
2a SECURITY CLASSIFICATION AUTHORITY			3 DISTRIBUTION AVAILABILITY STATEMENT approved for public release; distribution unlimited	
2b DECLASSIFICATION/DOWNGRADING SCHEDULE				
4 PERFORMING ORGANIZATION REPORT NUMBER(S)			5 MONITORING ORGANIZATION REPORT NUMBER(S)	
6a NAME OF PERFORMING ORGANIZATION Naval Postgraduate School		6b OFFICE SYMBOL (If applicable) PH	7a NAME OF MONITORING ORGANIZATION Naval Postgraduate School	
6c ADDRESS (City, State, and ZIP Code) Monterey, CA 93943-5000			7b ADDRESS (City, State, and ZIP Code) Monterey, CA 93943-5000	
8a NAME OF FUNDING/SPONSORING ORGANIZATION		8b OFFICE SYMBOL (If applicable)	9 PROCUREMENT INSTRUMENT IDENTIFICATION NUMBER	
8c ADDRESS (City, State, and ZIP Code)			10 SOURCE OF FUNDING NUMBERS	
			PROGRAM ELEMENT NO	PROJECT NO
			TASK NO	WORK UNIT ACCESSION NO
11 TITLE (Include Security Classification) Investigations of a Single Point Temperature Probe for Measurement of Atmospheric Turbulence				
12 PERSONAL AUTHOR(S) Hoover, Cloyes R. in conjunction with Donald L. Walters				
13a TYPE OF REPORT Master's thesis		13b TIME COVERED FROM TO	14 DATE OF REPORT (Year Month Day) December 1991	15 PAGE COUNT 72
16 SUPPLEMENTARY NOTES THE VIEWS EXPRESSED IN THIS THESIS ARE THOSE OF THE AUTHOR AND DO NOT REFLECT THE OFFICIAL POLICY OR POSITION OF THE DEPARTMENT OF DEFENSE OR THE U.S. GOVERNMENT.				
17 COSATI CODES			18 SUBJECT TERMS (Continue on reverse if necessary and identify by block number)	
FIELD	GROUP	SUB GROUP	Single point temperature probe, atmospheric optical turbulence, spatial coherence length, isoplanatic angle	
19 ABSTRACT (Continue on reverse if necessary and identify by block number) Gradients in the index of refraction caused by temperature fluctuations create optical turbulence. This optical turbulence greatly degrades the performance of imaging and laser systems operating in the atmosphere. There are several methods of measuring optical turbulence in the atmosphere, but few give a high resolution profile of the turbulence at all levels displaying the "layers" of turbulence that exist. This thesis is an investigation of the use of a high speed temperature probe coupled with a VIZ 9000 meteorological system to measure the optical turbulence in the atmosphere from a ground base to approximately 25 km. The processing of the data is done by a program developed as part of this research. The outputs of the program are $r_0$ , $\theta_0$ , $c_n^2$ as functions of altitude.				
20 DISTRIBUTION AVAILABILITY OF ABSTRACT <input checked="" type="checkbox"/> UNCLASSIFIED/UNLIMITED <input type="checkbox"/> SAME AS RPT <input type="checkbox"/> DTIC USERS			21 ABSTRACT SECURITY CLASSIFICATION unclassified	
22a NAME OF RESPONSIBLE INDIVIDUAL D. L. Walters			22b TELEPHONE (Include Area Code) (408) 646-2267	22c EXTENSION PH/We

Approved for public release; distribution is unlimited.

Investigations of a Single Point Temperature Probe  
For measurement of Atmospheric Turbulence

by

Cloyes R. Hoover  
Lieutenant, United States Navy  
B.S., University of Michigan, 1984

Submitted in partial fulfillment  
of the requirements for the degree of

MASTER OF SCIENCE IN PHYSICS

from the

NAVAL POSTGRADUATE SCHOOL  
December 1991

---

---

Department of Physics



## ABSTRACT

Gradients in the index of refraction caused by temperature fluctuations create optical turbulence. This optical turbulence greatly degrades the performance of imaging and laser systems operating in the atmosphere. There are several methods of measuring optical turbulence in the atmosphere, but few give a high resolution profile of the turbulence at all levels displaying the "layers" of turbulence that exist.

This thesis is an investigation of the use of a high speed temperature probe coupled with a VIZ 9000 meteorological system to measure the optical turbulence in the atmosphere from a ground base to approximately 25 km. The processing of the data is done by a program developed as part of this research. The outputs of the program are  $r_o$ ,  $\theta_o$ , and  $C_n^2$  as functions of altitude.

17053  
# 737  
2.1

# TABLE OF CONTENTS

I. INTRODUCTION	1
II. BACKGROUND	4
A. THEORY	4
B. SYSTEMS REQUIREMENTS	9
1. Processing System	9
2. Thermistor Probe	12
3. Computer Program	15
III. EXPERIMENTS	22
A. PROCEDURE	22
1. Maui Flights	22
2. NPS Flights	23
3. Mt. Wilson Flights	24
B. RESULTS	24
1. Maui Flights	24
2. NPS Flights	27

IV. CONCLUSIONS AND RECOMMENDATIONS . . . . .	31
A. CONCLUSIONS . . . . .	31
B. RECOMMENDATIONS . . . . .	32
APPENDIX A. PROGRAM FOR COMPUTING $C_n^2$ , $R_o$ , AND $\theta_o$ . . . . .	34
APPENDIX B. NOTES ON OPERATION OF VIZ-9000 SYSTEM . . . . .	45
APPENDIX C. PLOTS OF $C_n^2$ . . . . .	50
APPENDIX D. PROBE HEATING . . . . .	55
APPENDIX E. EFFECTS OF CONVERTING COUNTS TO RESISTANCE . . .	56
LIST OF REFERENCES . . . . .	63
INITIAL DISTRIBUTION LIST . . . . .	65





## I. INTRODUCTION

Since the Space Defense Initiative sparked a push to use laser weapons in space, many scientists have devoted their attention to the effects of propagating a laser beam (high power) through the atmosphere. The problems of propagating a laser beam in the atmosphere can be broken into four basic categories of detrimental effects [Ref. 1]. They are: absorption and scattering by atmospheric aerosols, stimulated Raman scattering, thermal blooming, and optical turbulence. It is important to note that all of these effects depend not only on the state of the atmosphere but also on the wavelength of the propagating beam and the mode of laser operation (CW or pulsed). Significant absorption of incident radiation induces thermal blooming when the absorbed energy alters the atmospheric index of refraction. At certain wavelengths, such as around  $3.8\text{ }\mu\text{m}$ , atmospheric "windows" exist where absorption is lower. Raman scattering is significant only when the peak power is sufficient to induce a nonlinear index of refraction in atmospheric nitrogen and oxygen, inducing higher order harmonics of the propagating wavelength [Ref. 1].

At shorter wavelengths atmospheric turbulence and scattering tend to dominate the beam propagation problem. Turbulence scrambles the phase of a laser beam across the wavefront, thereby spreading the energy over a larger solid angle ( $\mu$ radians to milliradians) than would be expected for a diffraction-

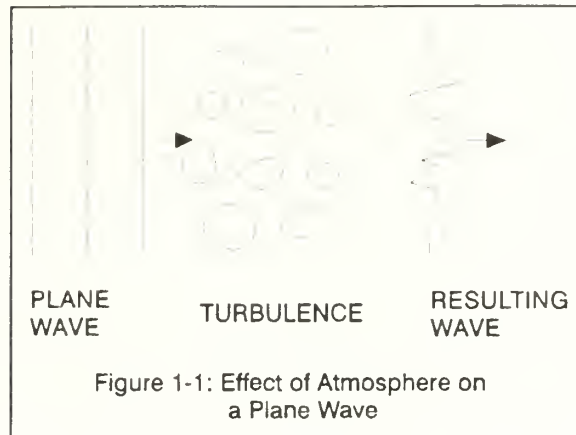
limited optical system. Scattering from aerosols spreads the energy over very large solid angles, on the order of one or more radians, which severely degrades collimation and reduces the beam energy that can be delivered to a small target.

When light propagates through a medium, the local phase of the wave depends on the product of the index of refraction of the medium ( $n$ ) and the path length between the source and the point in question. It is known that the index of refraction of our atmosphere at a given wavelength is not constant because atmospheric density is not constant. Some contributing factors are the decrease of density with altitude, differential heating by the sun, turbulent wind flow, and convection that causes localized inhomogeneities in the index of refraction, called optical turbulence (small variations in  $n$ ). The index of refraction in air is

$$n = 1 + 79 \times 10^{-6} \times \frac{P}{T} \quad (1)$$

where  $P$  is atmospheric pressure (millibars),  $T$  is temperature (kelvin), and the humidity term has been ignored since its contribution is so relatively small [Ref. 2]. Consequently, light that originates as a plane wave becomes a complex distorted wave after propagating a finite distance, as shown in figure 1-1 [Ref. 3].





There are several systems designed to measure optical turbulence. However, there is a need for a system that will produce a high resolution, accurate vertical profile of the turbulence verses altitude.

This thesis continues the development of a single point temperature thermosonde system to measure the vertical profile of the temperature structure parameter.

## II. BACKGROUND

### A. THEORY

From the arguments in the previous chapter, it is apparent that analysis of a laser system that propagates a beam from ground to space, or vice versa, requires an accurate understanding of atmospheric turbulence effects. Although these effects are random and complicated, statistical quantities can describe many of the relevant phenomena. A successful method that has been developed for such analysis uses structure functions to quantify the statistics of atmospheric turbulence (rather than autocovariance or autocorrelation functions). Wavefront phase distortion depends on localized differential variations in  $n$ , rather than upon those properties that are common to all portions of the wavefront. Therefore, structure parameters are inherently differential in form. A structure tensor as defined by Tatarski is [Ref. 2]:

$$D_{ij}(\overline{r_1}, \overline{r_2}) = \langle [ (f(\overline{r_1}) - \overline{f(\overline{r_1})}) - (f(\overline{r_2}) - \overline{f(\overline{r_2})}) ]^2 \rangle \quad (2)$$

where the angled brackets represent an ensemble average.

By making three assumptions [Ref. 4]:

- 1- Isotropy, so that only the magnitude of  $r$  is important, not the spatial orientation of the measurement
- 2- Homogeneity, which implies that a change in position does not alter the statistical properties of the turbulence
- 3- Incompressible turbulence

then:

$$D_f = \langle [f(r_1) - f(r_2)]^2 \rangle, \quad (3)$$

and

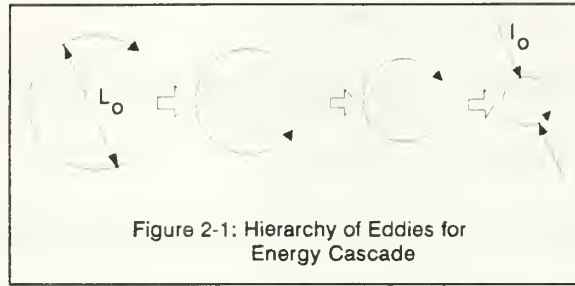
$$r = |\overline{r_1} - \overline{r_2}|. \quad (4)$$

Furthermore, by the Kolmogorov theory of turbulence, as long as  $r$  is within the "inertial subrange of turbulence" [Ref. 5], then

$$D_f = C_f^2 r^{2/3} \quad (5)$$

where  $C_f^2$  is a structure parameter. This inertial subrange of turbulence is the range from the small scale  $l_0$  of turbulence to the outer scale  $L_0$ . The small scale corresponds to the eddy size where viscous dissipation increasingly consumes the energy in the eddy. The outer scale corresponds to the largest scale size for which eddies can be considered still isotropic (see figure 2-1)[Ref. 4].





For temperature fluctuations that follow a Kolmogorov spectrum the temperature structure parameter  $C_T^2$  is [Ref. 2]

$$C_T^2 = \frac{\langle [T(r_2) - T(r_1)]^2 \rangle}{(r_2 - r_1)^{2/3}}, \quad (6)$$

where  $T$  is temperature (kelvin) and  $r$  is distance (meters).

Similarly the index of refraction structure parameter is [Ref. 2]

$$C_n^2 = \frac{\langle [n(r_2) - n(r_1)]^2 \rangle}{(r_2 - r_1)^{2/3}}, \quad (7)$$

where  $n$  is the index of refraction and  $r$  is distance (meters). Since atmospheric turbulence pressure fluctuations are small, the pressure term of the partial derivative of equation (1) is negligible, and  $C_n^2$  and  $C_T^2$  are related by the temperature partial derivative [Ref. 6]:

$$C_n^2 = (79 \times 10^{-6} \frac{P}{T^2})^2 C_T^2 \quad (8)$$

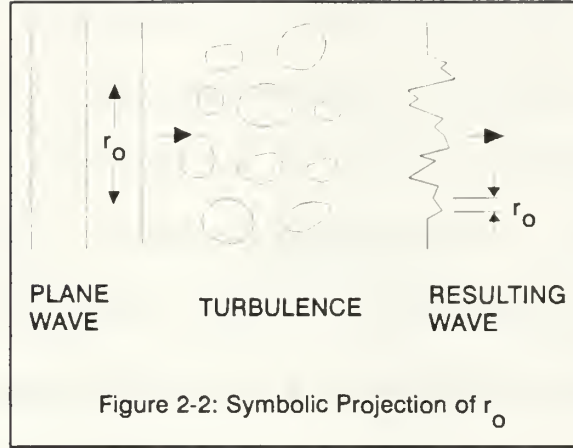
There are two statistical parameters that characterize the effect of optical turbulence. The first is  $r_0$ , which is a coherence length. It is a measure of

transverse spatial coherence of wave's electric field [Ref. 7]. In the absence of turbulence,  $r_o$  is comparatively large (see figure 2-2). The importance of  $r_o$  is that it describes the spatial resolution of an optical system. It is often called the "seeing parameter" or "Fried's parameter", and it determines the effective diffraction limit of an optical system. A large  $r_o$  is desirable if resolution is to be determined by the characteristics of the radiating aperture, rather than by turbulence.

In the absence of turbulence, the resolution of a diffraction-limited system is

$$\theta_D = \frac{a\lambda}{D} , \quad (9)$$

where  $\theta_D$  is the angular divergence of the beam (in radians),  $\lambda$  is the wavelength,  $D$  is the aperture size, and  $a$  is a geometric factor of order unity. Beam spread decreases with increasing aperture size  $D$ , until  $D$  reaches  $r_o$ . Further increase of  $D$  beyond  $r_o$  does not result in decreased beam divergence; the system's angular resolution stays constant.



Typical values for  $r_o$  are 5 cm (day) to 10 cm (night) for  $\lambda=500$  nm [Ref. 8]. For a plane wave,  $r_o$  depends upon the path integral of the index of refraction structure parameter,  $C_n^2$ . From Ref. 6

$$r_o = 2.1 [1.46 k^2 \int_0^L C_n^2(z) dz]^{-3/5} , \quad (10)$$

where  $k$  is the wave number. Equation 10 shows that  $r_o$  is proportional to  $\lambda^{6/5}$ .

Another related parameter is the isoplanatic angle,  $\theta_o$ . Whereas  $r_o$  is the spatial coherence length,  $\theta_o$  is the angular coherence length. It defines the "cone" in the atmosphere where turbulence is effectively the same for different angular paths. As with  $r_o$ , an optimized optical system should be characterized by a large  $\theta_o$ .  $\theta_o$  can be found by two methods. First it can be calculated by knowing  $C_n^2$  along an optical path [Ref. 9]:

$$\theta_o = [2.905 k^2 \int_0^L C_n^2(z) z^{5/3} dz]^{-3/5} , \quad (11)$$



where  $z$  is a path length in meters, or it can be measured by scintillation of starlight caused by random variations of local irradiance induced by turbulence [Ref. 4]. By use of equations 5 and 6, a balloon system with a high speed temperature probe can measure a profile of  $C_n^2$  from the ground to approximately 20 km above the earth. This profile can then be used to calculate  $\theta_o$ . Comparing optically measured  $\theta_o$  values to those computed from a balloon system will verify the accuracy of these measurements [Ref. 10].  $\theta_o$  also has a  $\lambda^{6/5}$  wavelength dependence. Typical values are 3-10  $\mu$ radians at  $\lambda = 500$  nm [Ref. 8].

Both  $r_o$  and  $\theta_o$  are measurable parameters that determine the effects of atmospheric turbulence that degrade the collimation and spatial coherence of a propagating electromagnetic wave. However,  $r_o$  and  $\theta_o$  are independent of each other. As equation 10 shows,  $r_o$  is equally weighted along the beam path.  $\theta_o$  is an indicator of higher altitude turbulence, however, as the  $z^{5/3}$  weighting in equation 11 suggests.

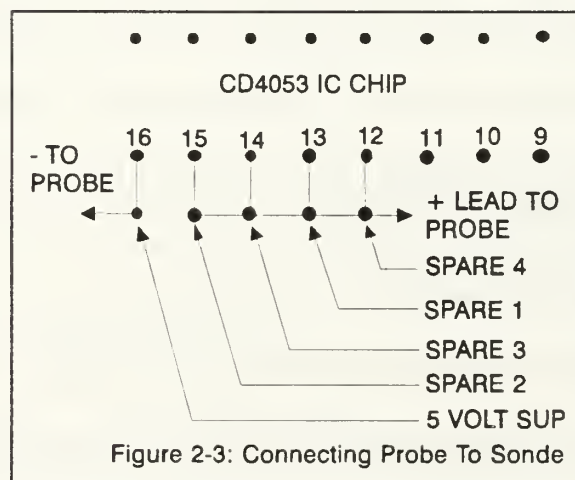
## **B. SYSTEMS REQUIREMENTS**

### **1. Processing System**

In 1989 the Naval Postgraduate School began development of a single point probe thermosonde system to obtain a  $C_T^2$  verses altitude profile. The main processing component of the system was a VIZ 9000 meteorological processing

system that utilizes VIZ 9000 digital Microsonde II thermosondes attached to weather balloons. The earlier version sonde (1543-364 Revx6) has 8 channels to collect data, but only 4 of these channels are used by the VIZ system for meteorological data collection. The remaining unused channels are used by the NPS group to measure the temperature of the atmosphere with a high speed thermistor probe; however, only 3 of these 4 channels were available for measuring temperature due to manufacturer design. Newer version sondes (1543-168B) now have all four spare channels available to measure temperature with an added probe.

The earlier NPS single point temperature probe systems used a 0.5 x 0.5 mm square Thermometrics thermistor flake. Since this thermistor proved to be too slow, this thesis concentrated on a faster probe [Ref. 10]. A 5 mil VECO thermistor probe (page 10) was connected to the thermosonde PC board as shown in figure 2-3.



The VIZ 9000 samples 8 channels every  $1.23 \pm 0.01$  second. These include a calibration signal, pressure, temperature, relative humidity and four spare channels (1 through 4). With the exception of the pressure channel, all of the measurements are resistances. The sampling time of each spare channel varies from 32 to 53 ms. The variable time is a consequence of an algorithm built into the MICROSONDE II sondes that compensates for the  $10^4$  to  $10^7$  range of resistance values normally encountered. The resistances measured by the system on the unused channels are stored into a computer file at the end of the flight and then are converted into temperatures.

System noise measurements of the older version VIZ microsonde II were done by NPS November 1990 [Ref. 10]. Table 1 is a summary of the measured system noise for the new version sondes. Fixed resistors were measured by the sonde giving total system noise expressed in terms of the standard deviation of the resistances and equivalent RMS temperatures.

TABLE 1. VIZ MICROSONDE II SYSTEM NOISE

Resistor	$\sigma$ (ch 1) ( $\Omega$ )	$\sigma$ (ch 2) ( $\Omega$ )	$\sigma$ (ch 3) ( $\Omega$ )	$\sigma$ (ch 4) ( $\Omega$ )
43 k $\Omega$	3.9 $\approx 0.005$ K	3.7 $\approx 0.005$ K	3.5 $\approx 0.005$ K	3.6 $\approx 0.005$ K
43 k $\Omega$	12.0 $\approx 0.008$ K	11.8 $\approx 0.008$ K	11.1 $\approx 0.008$ K	10.9 $\approx 0.008$ K
100 k $\Omega$	21.8 $\approx 0.007$ K	20.7 $\approx 0.007$ K	21.1 $\approx 0.007$ K	22.4 $\approx 0.007$ K
1 M	345 $\approx 0.012$ K	351 $\approx 0.012$ K	328 $\approx 0.012$ K	333 $\approx 0.012$ K

43 kΩ	12.0 ≈0.008 K	11.8 ≈0.008 K	11.1 ≈0.008 K	10.9 ≈0.008 K
100 kΩ	21.8 ≈0.007 K	20.7 ≈0.007 K	21.1 ≈0.007 K	22.4 ≈0.007 K
1 M	345 ≈0.012 K	351 ≈0.012 K	328 ≈0.012 K	333 ≈0.012 K

## 2. Thermistor Probe

After trying many different probes, the NPS group has had the most success with a 5 mil VECO thermistor probe. Figure 2-4 is a diagram of the construction of the probe. The response time of the probe was found to be

$$\frac{1}{\tau} = A + B\sqrt{V} \quad (12)$$

where  $\tau$  is the response time (sec), A and B are constants ( $A = 0.00758 \text{ msec}^{-1}$  and  $B = 0.0077 \text{ msec}^{-1} \cdot \text{sec}^{0.5}/\text{m}^{0.5}$ ), and  $v$  is the wind velocity (m/s) across the probe.

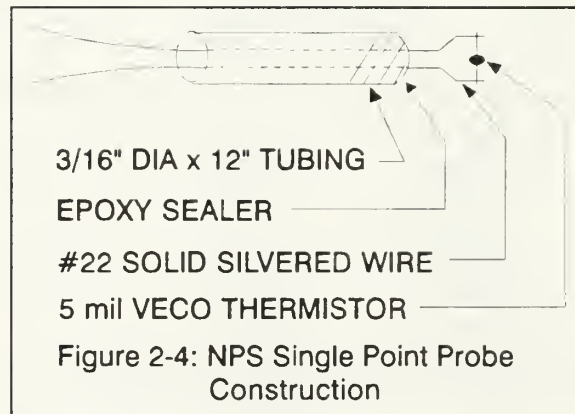


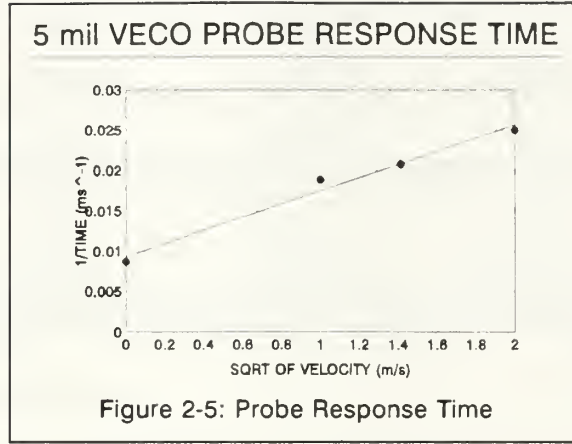


Figure 2-5 shows  $1/\tau$  versus  $v^{0.5}$  for wind velocities of 0, 1, 2 and 4 m/s measured in the lab with a chopped Halogen lamp illuminator as a heat source. The response time for the probe for an average ascent rate of 4 m/s was  $45 \pm 5$  msec.

To calibrate the probe, a method similar to the Steinhart-Hart equation [Ref. 11]

$$\frac{1}{T} = a + b\left(\ln \frac{r}{r_o}\right) + c\left(\ln \frac{r}{r_o}\right)^2 + d\left(\ln \frac{r}{r_o}\right)^3 \quad (13)$$

was found to work best by NPS in June 1990 where a, b, c, and d are coefficients and  $r_o$  room temperature resistance [Ref. 12]. The method uses an in flight calibration of the probe with the VIZ temperature sensor as a reference. A least squares algorithm computes the coefficients that are used to convert the thermistor resistances to temperatures.



The structure function used to calculate  $C_T^2$  in equation 6 is sensitive to the response time of the probe and the 32 - 53 msec integrating period of the A-D converter that is used in the VIZ system. Therefore the structure function over a limited scale length becomes [Ref. 11]:

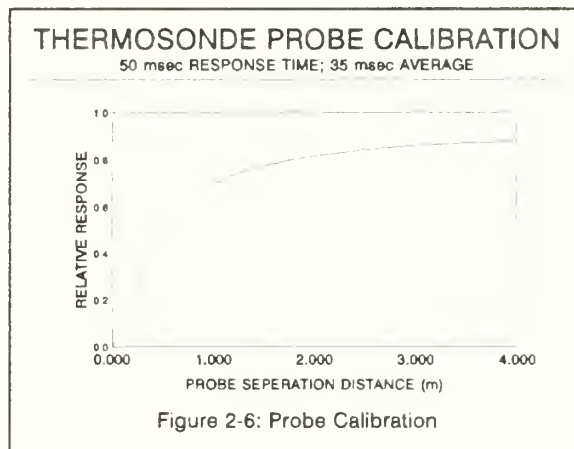
$$D(r, \tau_1, \tau_2) = 4 \int_a^b \sin^2\left(\frac{kr}{2}\right) k^{-5/3} \left[ \frac{\sin(k\tau_1/2)}{(k\tau_1/2)} \right]^2 \left[ \frac{1}{1 + (\omega\tau_2)^2} \right] dk \quad (14)$$

where  $a$  is  $2\pi/L_o$ , the limiting lower frequency (outer scale  $L_o$ ),  $b$  is  $2\pi/l_o$ , the limiting upper frequency (inner scale  $l_o$ ),  $k$  is  $2\pi/\lambda$ , the wave number,  $\tau_1$  is the A-D integrating time,  $\omega$  is  $kV$  where  $V$  is the wind velocity (thermosonde ascent rate), and  $\tau_2$  is the time constant of the temperature probe (the upper frequency cutoff).

The ratio of the filtered function to the ideal unfiltered structure function

$$\frac{D(r, \tau_1, \tau_2)}{D(r, 0, 0)} = \frac{D}{D_o} \quad (15)$$

gives the degradation to the calculation of  $C_T^2$  due to high frequency filtration by the probe. Figure 2-6 shows the correction required for different separation distances between temperature measurements for different probe separations.



### 3. Computer Program

The final component of the single point system is a computer program written in compiled QuickBASIC 4.5 that uses two converted binary to ASCII VIZ flight files as its input. The first file (flight.MTX) provides time, temperature, pressure, humidity, spare 1, spare 2, spare 3, and spare 4 resistance data. The second file (flight.MDX) provides time and altitude information.

A 21 point running mean is applied twice to the altitude data to remove the pressure sensor noise. Several different filtering methods were tried, with the double 21 point mean giving the best results as shown in figures 2-7 through 2-11. Next, the resistance data from all four spare channels were converted to temperature by the method discussed on page 12. The temperature differences from channel 1 to the next data measurement on channel 1 (spare 1-1) were calculated along with  $r$  (the distance between the measurements) and  $C_n^2$  was computed according to equation 6.  $C_n^2$  was next used to calculate  $r_o$  and  $\theta_o$ , using equations 8 and 9. This same procedure was repeated for temperature differences between channels 2 to 1, 3 to 1, and 4 to 1. Summarized, the times between temperature measurements were found as follows:

- 1) spare 1-1 =  $T_{1i} - T_{1i+1}$  ( $\approx 1.23$  sec apart)
- 2) spare 2-1 =  $T_{1i} - T_{2i}$  ( $\approx 0.05$  sec apart)
- 3) spare 3-1 =  $T_{1i} - T_{3i}$  ( $\approx 0.10$  sec apart)
- 4) spare 4-1 =  $T_{1i} - T_{4i}$  ( $\approx 0.15$  sec apart)

# SONDE TIME VS DELTA Z FLIGHT AF062622

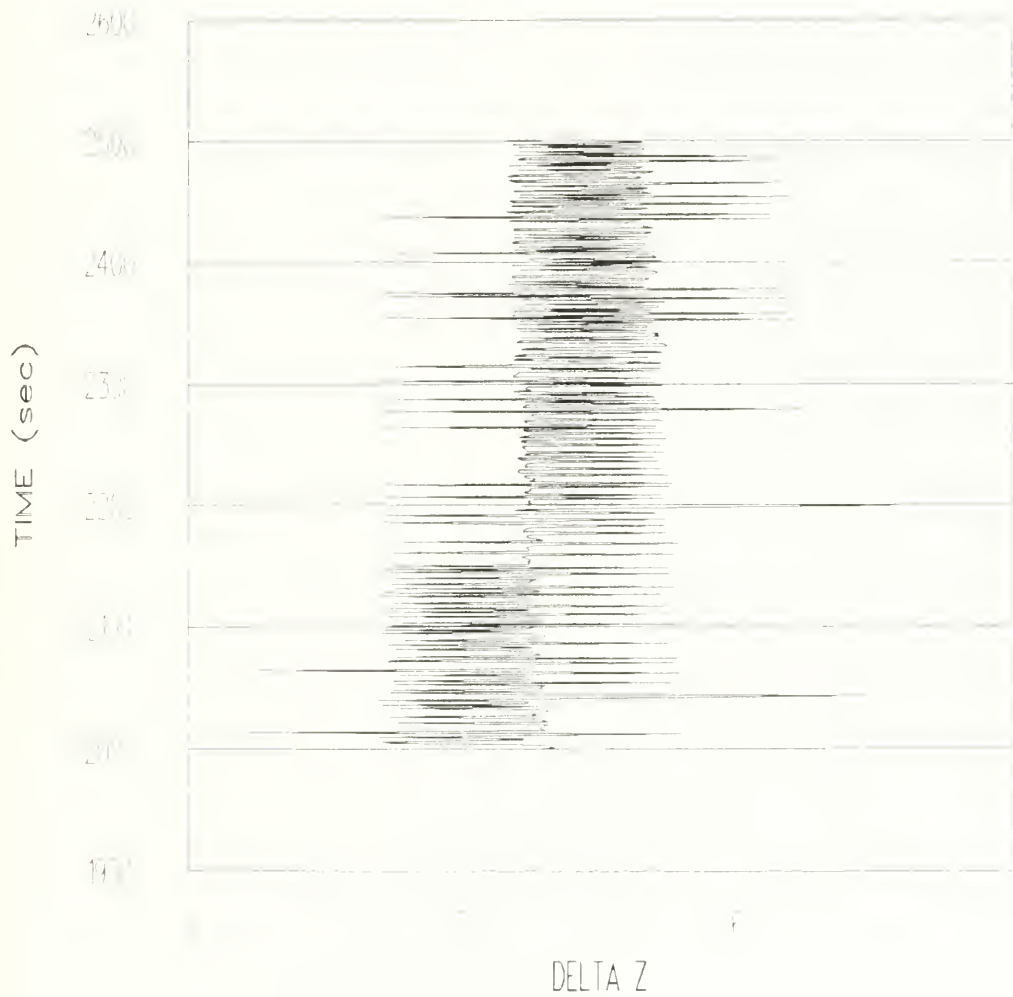


Figure 2-7: Effect of Noise in Pressure Sensor & Altitude Data



SONDE TIME VS DELTA Z  
FLIGHT AF062622  
5 POINT RUNNING MEAN OF ALTITUDE

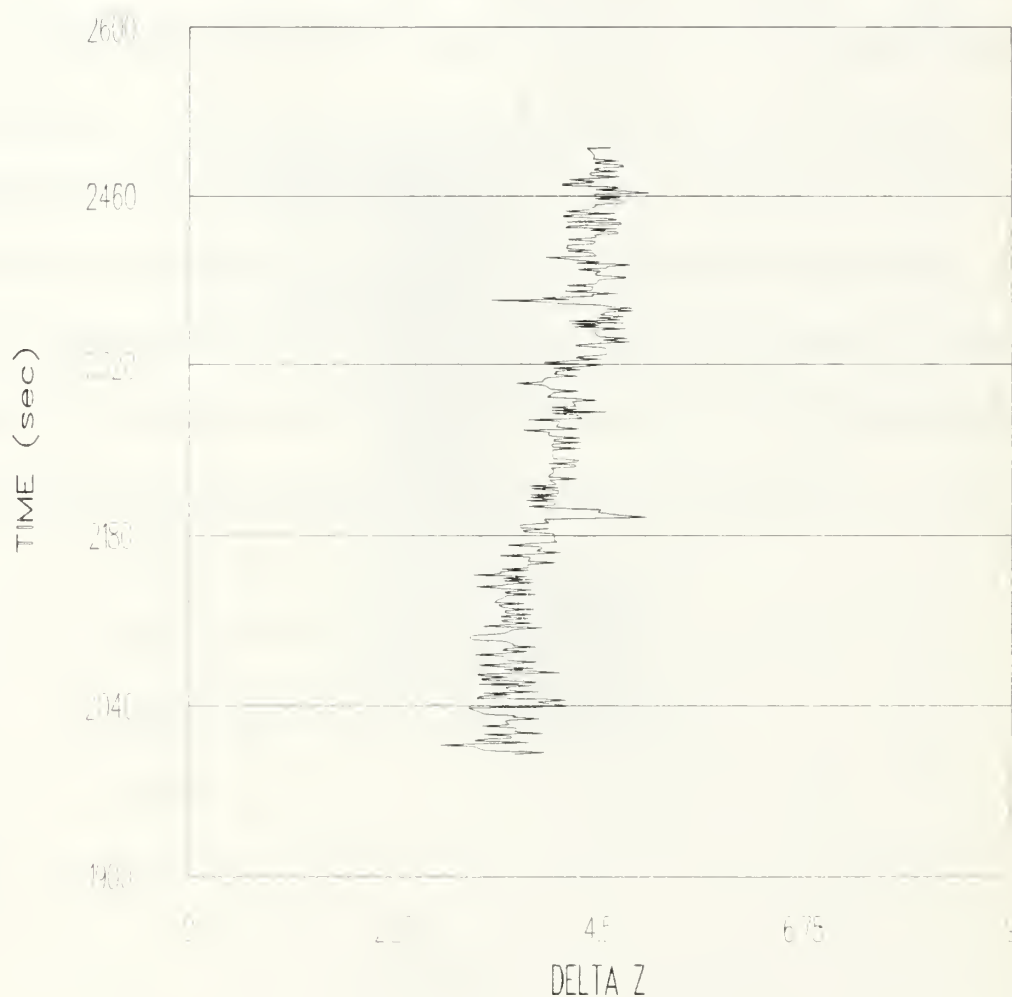


Figure 2-8: Effect of 5 Point Filter of Altitude Data

SONDE TIME VS DELTA Z  
FLIGHT AF062622  
20 POINT RUNNING MEAN OF ALTITUDE

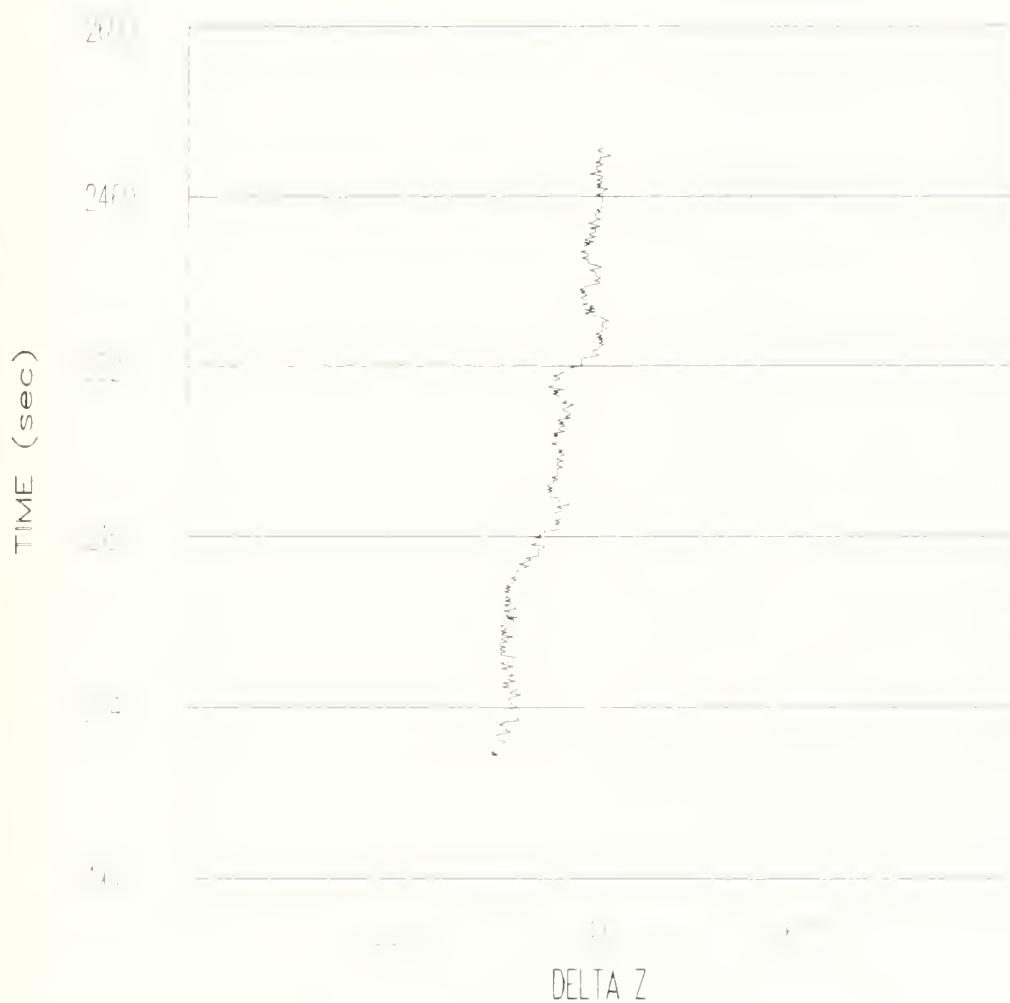


Figure 2-9: Effect of 21 Point Filter of Altitude Data

SONDE TIME VS DELTA Z  
FLIGHT AF062622  
31 POINT RUNNING MEAN OF ALTITUDE

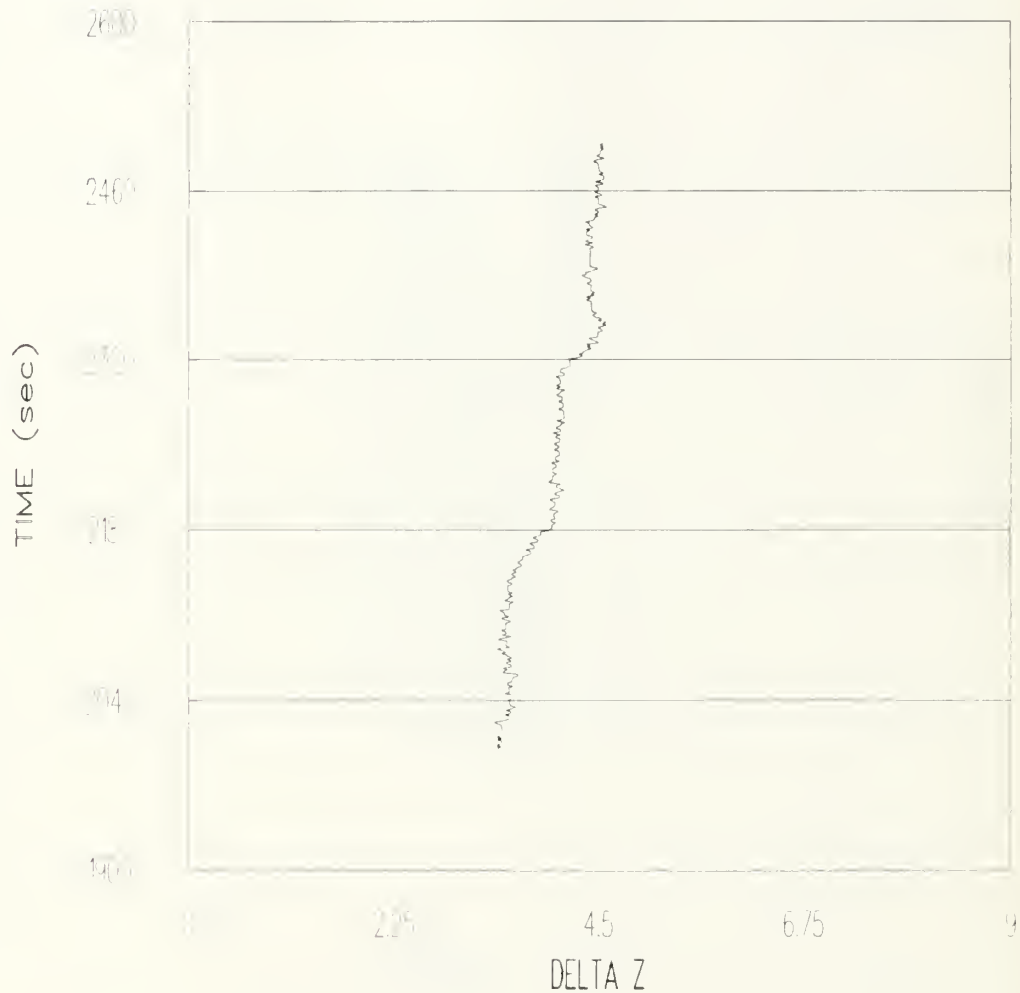


Figure 2-10: Effect of 31 Point Filter of Altitude Data

SONDE TIME VS DELTA Z  
 FLIGHT AF062622  
 21 POINT RUNNING MEAN OF ALTITUDE  
 DOUBLE FILTER



Figure 2-11: Effect of Double 21 Point Filter

### III. EXPERIMENTS

#### A. PROCEDURE

##### 1. Maui Flights

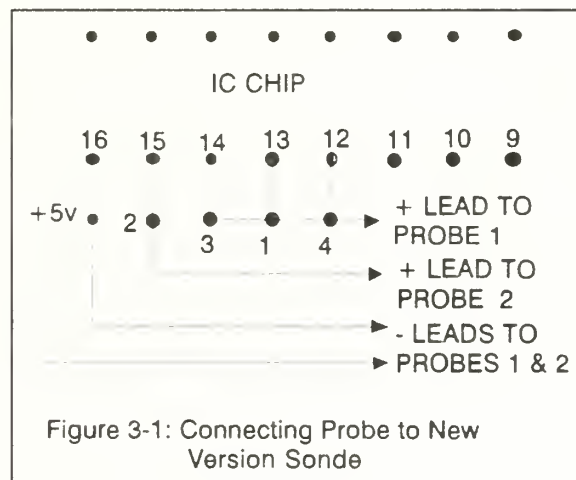
The mission of the Maui trip was to aid in site selection for a proposed Air Force, 4 meter telescope to be installed. A series of acoustic sounder measurements and balloon launches occurred at the Air Force Maui Observation Station (AMOS), Haleakala, Hawaii between 26 June to 2 July 1991 [Ref. 13]. Additionally, the 1.6 meter telescope with the Itek Compensated Imaging System (CIS) at AMOS gathered stellar image full width half maximum data. The NPS group also launched single point probe thermosonde systems on 28, 29, and 30 June 1991. The 28 and 29 June flights used the newer (168B) Microsonde II sondes, while the 30 June flight used the older version (Rev X-6) sonde.

All three thermosonde flights were launched after sunset (approximately 2200 local time) to avoid solar heating of the probes [Ref. 10]. At the time of launch, the NPS group did not know the new version sondes (28 and 29 June) had different electronic configurations than the older version sondes, therefore the probe wiring was connected similarly to the previous sondes. This became a problem because a resistance voltage divider and diode had been added to the circuit connected across spare channel 4 to monitor the sonde battery voltage; the 30 June flight however, being an older version sonde

used in previous NPS work, did not include this circuitry. Although the resistance divider and diode contaminated the results, particularly at higher altitudes where the resistances are in the 100k to 1M range, the lower altitude data was not contaminated excessively.

## 2. NPS Flights

The NPS group measured  $\theta_0$  optically 15 November 1991 from 2130 to 2330 local time. A thermosonde system was launched from the roof of the Naval Postgraduate School's Spanagel Hall during this same period. The sonde was a new version Microsonde II with the voltage divider and diode removed, however this launch included two probes as shown in figure 3-1.



Two thermistor probes connected to channel 1 and channel 2 respectively and separated by 1m provided a fixed separation distance between probes. This provided a means to compute horizontal differential temperature measurements.



### 3. MT. Wilson Flights

In support of characterization measurements of Mt. Wilson, California, three balloon launches occurred in September 1991. None of these yielded useful data, since RF interference on Mt. Wilson contaminated the measurements. The Loran and Omega navigational aid systems used to determine the sondes' location for determination of wind data were particularly susceptible to the interference.

## B. RESULTS

### 1. Maui Flights

Table 2 shows the results of the thermosonde flights for 28, 29, and 30 June 1991 (one flight per night) in comparison with the acoustic sounder data and the AMOS 1.6 m telescope data (their measurement of  $r_o$  at the time of the balloon flight).

A 5 point running mean of the temperature data was used in the thermosonde  $C_T^2$  program and then corrected as shown on page 13.

TABLE 2. CORRECTED  $R_o$  (cm) COMPARISON MEASUREMENTS

DATE	AMOS	NPS	1-1	3-1	4-1	AVE
28 JUN		10-11	3.9	3.1	3.3	3.4
29 JUN	7-8	9-10	2.26	2.25	2.29	2.27
30 JUN	9-10		8.9		7.0	7.95

The flights on the 28 and 29 June differed from the other systems by a factor of three. This is believed to be due to the diode circuit in spare channel 4 (new version sondes). The 30 June flight (old version sonde) shows agreement with the AMOS 1.6 m CIS measurements within 12% discussed in Reference 13.

A problem exists when computing vertical temperature differences. Since the mean atmospheric temperature changes rapidly with altitude, vertical temperature differences  $\langle (T(z_2) - T(z_1))^2 \rangle$  contain some unavoidable mean value changes that are not induced by turbulence. This phenomena is particularly prominent as the sensors cross a sharp temperature inversion. This thesis considered a variety of running means to remove the  $T_2 - T_1$  mean. Figures 3-2 and 3-3 show the effect of 5 to 21 point running means on the computation of  $R_o$  and  $\theta_o$ .

Figure 3-2 shows a monotonic increase in  $r_o$  as the length of the running mean becomes shorter. This demonstrates that there may be no acceptable running mean length and other reduction techniques may be necessary. From figure 3-2 it is apparent that the channel 4-1 measurements are much less sensitive to the form of the running mean. This is simply a consequence of the short time period and distance between measurements. The channel 1-1 measurements are widely separated and are inherently sensitive to gradients in temperature. In table 2 the channel 4-1 measurements are the most accurate. The channel 1-1 measurements in table 2 have been artificially enhanced by the 5 point running mean compared to the 21 point results.

Another source of systematic errors present when differencing channel 1 and channels 3 or 4 are the fluctuations in time measurements from channel 1 to 3 and 1 to 4. To calculate the separation distance  $r$  used in equation 10, an average of 100 msec and 150 msec time was used in the program. However, the signal time occasionally varies by as much as 10% . This leads to noise in the separation distance for channels 3-1 and 4-1 that is not present for channel 1-1 differencing.

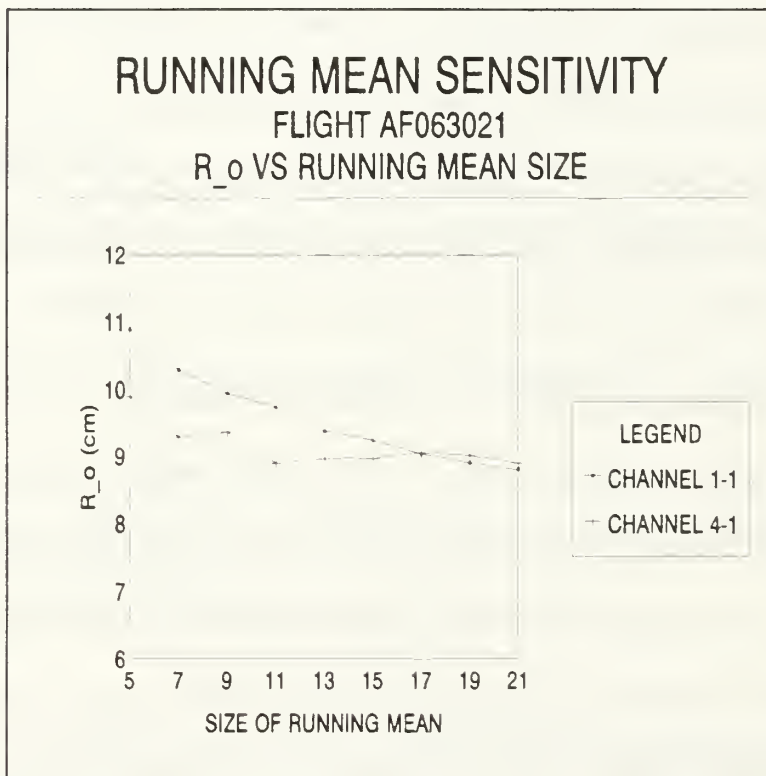


Figure 3-2: Running Mean Sensitivity

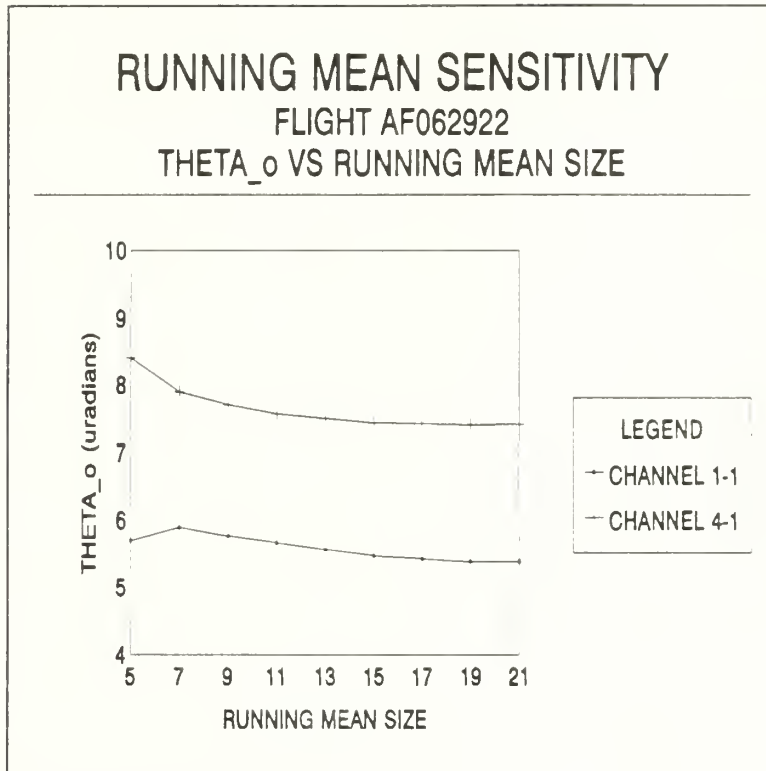


Figure 3-3: Running Mean Sensitivity

## 2. NPS Flight

Table 3 shows the results of the thermosonde flight done on 15 November 1991 compared to optical measurements of the isoplanatic angle. The dual point probe and optical measurement method agreed very well, while the single point probe are 13% smaller than the optical measurement.

TABLE 3. CORRECTED  $\theta_o$  ( $\mu$ radians) COMPARISON MEASUREMENTS

DATE	OPTIC	DUAL	1-1	3-1	4-1	AVE
15 NOV	3-4	3.3	3.1	2.2	2.4	2.6

Tables 2 and 3 suggest that the sonde circuitry may be inducing extraneous noise in the data. The VIZ 9000 MICROSONDE II sondes measure resistance by counting clock pulses of an oscillator circuit [Ref. 10]. These clock pulses (counts) are then converted to resistance by the manufacturers software that is part of the VIZ system. To maintain high resistance and temperature resolution (0.002 to 0.008 K), the sonde alters the measurement period by factors of two to keep the counts in the  $2^{15}$  to  $2^{16}$  range. It was found that this altering or "ratcheting" happened at approximately the 60 and 260 k $\Omega$  resistance measurements. This has an unfortunate side effect on the small thermistor probe self heating. Ohmic heating of the thermistor is proportional to the power dissipated by the probe as well as the time duration of the probe current. Figure 3-4 shows a ratcheting effect in the channel 2 minus channel 1 temperature differences at the 60 k $\Omega$  shift point. A consistent shift of 0.5 K occurs above 7300 m in the temperature differences as the sonde shifts to a shorter count interval. Significant temperature spikes on the order of 0.05 K occur between 7100 and 7300 m.

These fluctuations appear to be the result of an instability near the threshold point, as if the sonde shifts periods back and forth several times before stabilizing. This effect induces a false turbulence signal in the isoplanatic angle on the order of 5-10%.

This phenomena appears in every sonde launch investigated to date when the sonde clock circuitry shifts averaging times. Appendix E includes a series of plots that further demonstrates this effect. Surprisingly, the "stutter" effect appears in the temperature differences but not in the raw counts recorded by the system. It is clear that channels 5-8 each shift periods at different times. The cause of this phenomenon is not completely understood at this time and should be investigated.



FLIGHT AF063021  
ALTITUDE VS DELTA T  
CHANNEL 4-1

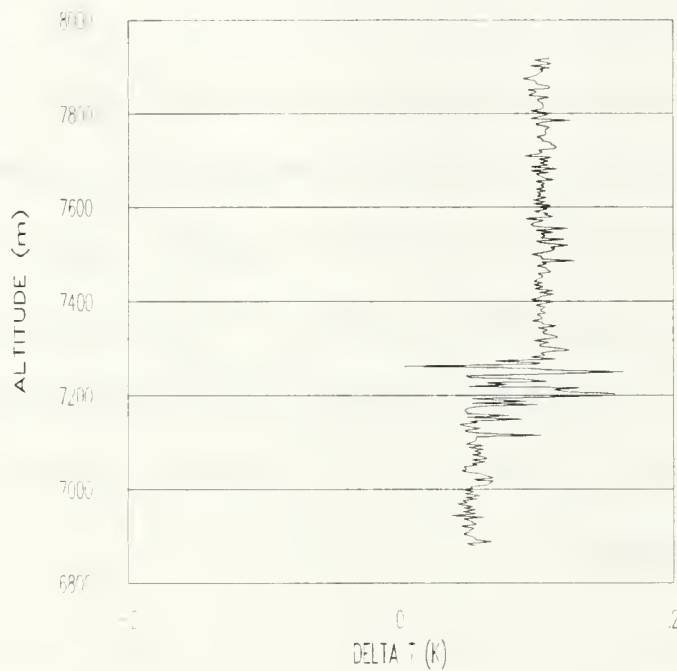


Figure 3-4: Ratcheting Effect on Delta T

## IV. CONCLUSIONS AND RECOMMENDATIONS

### A. CONCLUSIONS

The new high speed 5 mil VECO thermistor probe proved to be a large improvement in the single point probe method of measuring atmospheric turbulence. The results of measurements of  $r_o$  and  $\theta_o$  are now within 10 to 12 percent of the other methods of measuring the turbulence.

The new version sondes are more useful than the older version by allowing the use of all 4 spare channels for data collection. The noise in the new version sonde is consistent with what was measured in the old version, therefore the noise filtering methods used for the old sondes are the same for the new version sondes. A successful method of filtering the altitude data was found to be a double 21 point running mean.

This thesis found that a running mean applied to first order temperature differences was not sufficient for trend removal. Coherence length computed with 5-21 point running means showed a monotonic increase for shorter running means. It appears that no running mean is suitable. Other data reduction techniques will be necessary.

Systematic spikes in Microsonde II temperature data were found near the resistance range change points. These temperature spikes contaminated the isoplanatic angle by 10%. They will have to be removed by software or hardware modifications in future work.

The improved high speed thermistor, along with the new version sonde and a computer program incorporating altitude filtering and high order temperature differencing will allow the NPS group to have a working single point probe system. This system has the ability to plot altitude verses  $C_n^2$  displaying where the layers of optical turbulence are encountered.

## **B. RECOMMENDATIONS**

To gain more confidence in the filtering methods used in the computer program and to establish a statistical data base for measurement comparisons, a number of flights should be launched with the two point probe system. These obviously should cover a wide range of both "good seeing" and "poor seeing" days. Another advantage of doing numerous flights to establish a data base is that a calibration correction factor could then be applied to the 3-1 and 4-1 channels.

A continued study of how to handle the temperature inversions with a signal filter needs to be carried out and incorporated into the computer program. This is probably the future research area that would produce the greatest improvement to the system.

It is unknown if the variations in the timing intervals between channel 1 to 4 can be handled or removed well enough to bring into agreement measurements across all channels. If the noise is not improved, then output measurements should be restricted to differencing channel 1-1 for a single point probe or 2-1 for a dual point probe.

Shortening the time between scans is a hardware improvement to the VIZ Microsonde II that will improve performance. If this scan interval could be shortened from the present 1.23 sec to approximately 0.5 sec with the same low noise, it would be a big improvement for use as a single point system. This is because 0.15 sec tends to be too short for a 50 ms probe response time, while 1.23 sec is too long (which corresponds to  $\approx 5$  m spacing). Therefore 0.5 sec ( $\approx 2$  m spacing) should improve the measurements.

## APPENDIX A. PROGRAM FOR COMPUTING $C_n^2$ , $R_o$ , AND $\theta_o$

```

DECLARE SUB Crout (a!(), b!(), c!)
DECLARE FUNCTION temp! (r!, b!())
DEFINT I-N
OPTION BASE 1
DIM xm(0 TO 10)
DIM a(4, 4), b(4)
' This program reads the ASCII .mtx and .mdx file created by
' the VIZ 9000 SYSTEM and performs a least squares fit
' creating a temperature data output.
' It then filters the altitude data and computes  $CN^2$ ,  $R_o$ , and
'  $\theta_o$  for 4 spare channels of data from the temperature
' data creating an altitude verses  $CN^2$  output file to be
' plotted with SUPERCALC.
' DLW Sep 11 1990 (temperature conversion program)
' CRH Nov 10 1991
' To declare dynamic data array, invoke Quickbasic with /ah
' option

' LIST OF VARIABLES AND CONSTANTS:
' start = starting altitude data point    ro1=  $R_o$  for spare 1-1
' stp = stopping altitude data point      Oo1=  $\theta_o$  for
                                           spare 1-1
' dta(i,1)= time (sec)                    ro2=  $R_o$  for spare 2-1
' dta(i,2)= pressure (mbar)                Oo2=  $\theta_o$  for
                                           spare 2-1
' dta(i,3)= VIZ temp (C)                   ro3=  $R_o$  for spare 3-1
' dta(i,4)= humidity (%)                   Oo3=  $\theta_o$  for
                                           spare 3-1
' dta(i,5)= spare 1 resistance & temp (K)
' dta(i,6)= spare 2 resistance & temp (K)
' dta(i,7)= spare 3 resistance & temp (K)
' dta(i,8)= spare 4 resistance & temp (K)
' dta(i,9)= VIZ altitude (m)
' dta(i,10)= first 21 pt mean altitude
' dta(i,11)= 2nd 21 pt mean altitude
' dta(i,12)= delta T for all spares (reused)
' dta(i,13)= mean delta T for all spares (reused)
' dta(i,14)=  $CN^2$  for spare 1-1            ro4=  $R_o$  for spare 4-1
' dta(i,15)=  $CN^2$  for spare 2-1            Oo4=  $\theta_o$  for
' dta(i,16)=  $CN^2$  for spare 3-1            spare 4-1
' dta(i,17)=  $CN^2$  for spare 4-1
' b(1)= coefficient of polynomial to convert resistance to
        temperature
' b(2)= , ,

```

```

' b(3)= coefficient of polynomial to convert resistance to
      temperature
' b(4)= , ,
' low = number of data pts lost due to running mean size
' high = number of data pts lost due to running mean size at
        end of flight for spare 1-1 only.
' ST = desired starting altitude
' RM = desired running mean size
' pts = number of vertical data points

REM $DYNAMIC
DIM dta(6000, 17)

tzero = 273.15                      ' zero Celcius

INPUT "enter MTX filename "; MTX$

PRINT
PRINT MTX$
OPEN MTX$ FOR INPUT AS #1

INPUT "enter MDX filename "; MDX$

PRINT
PRINT MDX$
OPEN MDX$ FOR INPUT AS #2

l = 0
DO UNTIL EOF(1)
  l = l + 1
  INPUT #1, dta(l, 1), dta(l, 2), dta(l, 3), dta(l, 4),
    dta(l, 5), dta(l, 6), dta(l, 7), dta(l, 8)
LOOP

l = 0
DO UNTIL EOF(2)
  l = l + 1
  INPUT #2, x, y, dta(l, 9)  'x and y are unneeded variables
LOOP

'FIND START AND STOP OF FLIGHT

N = 1
FOR i = 1 TO (N / 2)
  IF (dta(i, 9) < dta(i + 1, 9)) AND
    (dta(i + 1, 9) < dta(i + 2, 9)) AND
    (dta(i + 2, 9) < dta(i + 3, 9)) AND
    (dta(i + 3, 9) < dta(i + 4, 9)) AND
    (dta(i + 1, 9) - dta(i, 9)) > 2 AND

```



```

    (dta(i + 2, 9) - dta(i + 1, 9)) > 2
THEN GOTO 10
    NEXT i

10 start = i      'exited loop when conditions were met

FOR i = N TO (N / 2) STEP -1
    IF dta(i, 9) > dta(i - 1, 9) AND
        dta(i - 1, 9) > dta(i - 2, 9) AND
        dta(i - 2, 9) > dta(i - 3, 9) THEN GOTO 20
    NEXT i
20 stp = i      'exited loop when conditions were met

CLOSE #1: CLOSE #2

'CORRECT ALTITUDE (VIZ MAX ALTITUDE INPUT IS 2500 m)

INPUT "enter altitude correction (m)"; zcor
PRINT
PRINT zcor
FOR i = start TO stp
    dta(i, 9) = dta(i, 9) + zcor
NEXT i

'DO DOUBLE 21 PT RUNNING MEAN ON ALTITUDE (Z)

'first 21 point mean
FOR i = start TO (stp - 20)
    num! = 0!
    FOR j = i TO (i + 20)
        num! = num! + dta(j, 9)
    NEXT j
    dta(i + 10, 10) = num! / 21!
NEXT i

'second 21 point mean
FOR i = (start + 10) TO (stp - 30)
    num! = 0!
    FOR j = i TO (i + 20)
        num! = num! + dta(j, 10)
    NEXT j
    dta(i + 10, 11) = num! / 21!
NEXT i

' compute average ascent distance between data points at start
' of flight

zlave! = (dta(start + 24, 11) - dta(start + 20, 11)) / 4!

```

```

' compute average ascent distance between data points at end
' of flight

z2ave! = (dta(stp - 20, 11) - dta(stp - 24, 11)) / 4!

' compute averaged altitudes to fill in first 20 data pts lost
' by double filter

FOR j = 1 TO 20
    dta(j, 11) = dta(start + 20, 11) - ((21 - j) * (z1ave!))
NEXT j
j = 1
FOR i = start TO (start + 19)
    dta(i, 11) = dta(j, 11)
    j = j + 1
NEXT i

' compute averaged altitudes to fill in last 20 data pts lost
' by double filter

FOR j = 1 TO 20
    dta(j, 11) = dta(stp - 20, 11) + (j * z2ave!)
NEXT j

j = 1

FOR i = (stp - 19) TO stp
    dta(i, 11) = dta(j, 11)
    j = j + 1
NEXT i

' The following is a program to convert resistance data to
' temp data

' begin least squares fit

m = 4
FOR i = 1 TO m
    FOR j = 1 TO m
        a(i, j) = 0!
    NEXT j
    b(i) = 0!
NEXT i

m2 = m + m - 2
FOR k = start TO stp
    xk = LOG(dta(k, 5))
    yk = 1! / (dta(k, 3) + tzero)

    xm(0) = 1!

```

```

FOR i = 1 TO m2
    xm(i) = xk * xm(i - 1)          ' xm = x^m
NEXT i

FOR i = 1 TO m
    i2 = i - 2
    FOR j = i TO m
        a(i, j) = a(i, j) + xm(i2 + j)    ' x^(i-1+j-1)
    NEXT j
    b(i) = b(i) + yk * xm(i - 1)
NEXT i

NEXT k

' set lower half of matrix

FOR i = 1 TO m
    FOR j = 1 TO i
        a(i, j) = a(j, i)
    NEXT j
NEXT i

c = m
CALL Crout(a(), b(), c)

PRINT b(1), b(2), b(3), b(4)

' convert to temperature

FOR i = start TO stp
    dta(i, 3) = dta(i, 3) + tzero
    resistance = dta(i, 5)
    dta(i, 5) = temp(resistance, b())
    resistance = dta(i, 6)
    dta(i, 6) = temp(resistance, b())
    resistance = dta(i, 7)
    dta(i, 7) = temp(resistance, b())
    resistance = dta(i, 8)
    dta(i, 8) = temp(resistance, b())
NEXT i

'RENUMBER ARRAY FROM 1 TO N

FOR i = start TO stp
    FOR j = 1 TO 11
        dta(i + 1 - start, j) = dta(i, j)
    NEXT j
NEXT i
N = (i - start + 1)
PRINT

```

```

PRINT "starting altitude = "; dta(1, 11)
PRINT "stopping altitude = "; dta(N, 11)

' allow user to select new starting altitude to examine
' portion of flight

PRINT
INPUT "enter new desired starting altitude"; ST
PRINT
PRINT ST

FOR i = 1 TO N
  IF dta(i, 11) > ST THEN GOTO 30
NEXT i
30 start = i
PRINT
PRINT "New starting altitude = "; dta(start, 11)

' compute number of data points

stp = N
pts = stp - start + 1
PRINT
PRINT "number of data points are "; pts

'ENTER RUNNING MEAN TO BE USED FOR dT

INPUT "enter size of running mean (odd number) for temp"; RM
PRINT
PRINT "dT running mean is "; RM

'COMPUTE CT^2 FOR SPARE 1 - SPARE 1 TEMP DIFFERENCE

'COMPUTE DELTA T

FOR i = start TO (stp - 1)
  dta(i, 12) = dta(i, 5) - dta(i + 1, 5)
NEXT i

'DO RUNNING MEAN OF dT

low = (RM - 1) / 2
high = (RM + 1) / 2
FOR i = start TO (stp - RM)
  num! = 0!
  FOR j = i TO (i + RM - 1)
    num! = num! + dta(j, 12)
  NEXT j
  dta(i + low, 13) = num! / RM!
NEXT i

```

```

'compute cn2

FOR i = (start + low) TO (stp - high)
  dta(i, 14) = (((.000079 * dta(i, 2)) / (dta(i, 3) ^ 2)) ^ 2) *
    ((dta(i, 12) - dta(i, 13)) ^ 2) / ((dta(i + 1, 11)
      - dta(i, 11)) ^ (.6667))
NEXT i
h! = 2.1 * (1.46 * (2 * 3.14159 / 500E-09) ^ 2) ^ -0.6
sum! = 0!

' compute Ro (CN^2 * dz)

FOR i = (start + low) TO (stp - high)
  sum! = sum! + ((dta(i + 1, 11) - dta(i, 11)) * dta(i, 14))
    'dz=dta(i+1,11)-dta(i,11)
NEXT i
sum2! = sum! ^ (-.6)
rol! = h! * sum2!

'COMPUTE Oo for 1-1 (CN^2 * dz * z^5/3)

f! = (2.905 * (2 * 3.14159 / 500E-09) ^ 2) ^ -0.6
sumO! = 0!
FOR i = (start + low) TO (stp - high)
  sumO! = sumO! + (((dta(i + 1, 11) - dta(i, 11)) *
    dta(i, 14)) * (dta(i, 11) - dta(start, 11)) ^ 1.6667)
NEXT i
sumO2! = sumO! ^ (-.6)
Ool! = f! * sumO2!

'COMPUTE CT^2 FOR SPARE 2 - SPARE 1 TEMP DIFFERENCE

'compute delta T

FOR i = start TO stp
  dta(i, 12) = dta(i, 5) - dta(i, 6)
NEXT i

'do running mean of dT

FOR i = start TO (stp - RM + 1)
  num! = 0!
  FOR j = i TO (i + RM - 1)
    num! = num! + dta(j, 12)
  NEXT j
  dta(i + low, 13) = num! / RM!
NEXT i

'compute cn2

```

```

FOR i = (start + low) TO (stp - low)
  dta(i, 15) = (((.000079 * dta(i, 2)) / (dta(i, 3) ^ 2)) ^ 2) *
    ((dta(i, 12) - dta(i, 13)) ^ 2) / (((dta(i + 1, 11)
      - dta(i, 11)) / 1.23) * .05) ^ (.6667))
NEXT i
sum! = 0!
sum2! = 0!
FOR i = (start + low) TO (stp - low)
  sum! = sum! + (dta(i, 15) * (dta(i + 1, 11) - dta(i, 11)))
NEXT i
sum2! = sum! ^ (-.6)
ro2! = h! * sum2!

'compute Oo for 2-1

sumO! = 0!
FOR i = (start + low) TO (stp - low)
  sumO! = sumO! + (((dta(i + 1, 11) - dta(i, 11)) *
    dta(i, 15)) * (dta(i, 11) - dta(start, 11)) ^ 1.6667)
NEXT i
sumO2! = sumO! ^ (-.6)
Oo2! = f! * sumO2!

'COMPUTE CT^2 FOR SPARE 3 - SPARE 1 TEMP DIFFERENCE

'compute dT

FOR i = start TO stp
  dta(i, 12) = dta(i, 5) - dta(i, 7)
NEXT i

'compute running mean of dT

FOR i = start TO (stp - RM + 1)
  num! = 0!
  FOR j = i TO (i + RM - 1)
    num! = num! + dta(j, 12)
  NEXT j
  dta(i + low, 13) = num! / RM!
NEXT i

'compute cn2

FOR i = (start + low) TO (stp - low)
  dta(i, 16) = (((.000079 * dta(i, 2)) / (dta(i, 3) ^ 2)) ^ 2) *
    ((dta(i, 12) - dta(i, 13)) ^ 2) / (((dta(i + 1, 11)
      - dta(i, 11)) / 1.23) * .1) ^ (.6667))
    'dz/1.23= vel'y
    'r=vel'y * 0.1sec
NEXT i

```



```

sum! = 0!
sum2! = 0!
FOR i = (start + low) TO (stp - low)
    sum! = sum! + (dta(i, 16) * (dta(i + 1, 11) - dta(i, 11)))
NEXT i
sum2! = sum! ^ (-.6)
ro3! = h! * sum2!

'compute Oo for 3-1

sumO! = 0!
FOR i = (start + low) TO (stp - low)
    sumO! = sumO! + (((dta(i + 1, 11) - dta(i, 11)) *
        dta(i, 16)) * (dta(i, 11) - dta(start, 11)) ^ 1.6667)
NEXT i
sumO2! = sumO! ^ (-.6)
Oo3! = f! * sumO2!

'COMPUTE CT^2 FOR SPARE 4 - SPARE 1 TEMP DIFFERENCE

'compute delta T

FOR i = start TO stp
    dta(i, 12) = dta(i, 5) - dta(i, 8)
NEXT i
FOR i = start TO (stp - RM + 1)
    num! = 0!
    FOR j = i TO (i + RM - 1)
        num! = num! + dta(j, 12)
    NEXT j
    dta(i + low, 13) = num! / RM!
NEXT i

'compute cn2

FOR i = (start + low) TO (stp - low)
    dta(i, 17) = (((.000079 * dta(i, 2)) / (dta(i, 3) ^ 2)) ^ 2) *
        ((dta(i, 12) - dta(i, 13)) ^ 2) / (((dta(i + 1, 11)
        - dta(i, 11)) / 1.23) * .15) ^ (.6667))
NEXT i
sum! = 0!
sum2! = 0!
FOR i = (start + low) TO (stp - low)
    sum! = sum! + dta(i, 17) * (dta(i + 1, 11) - dta(i, 11))
NEXT i
sum2! = sum! ^ (-.6)
ro4! = h! * sum2!

'COMPUTE Oo for 4-1

```

```

sumO! = 0!
FOR i = (start + low) TO (stp - low)
    sumO! = sumO! + (((dta(i + 1, 11) - dta(i, 11)) *
        dta(i, 17)) * (dta(i, 11) - dta(start, 11)) ^ 1.6667)
NEXT i
sumO2! = sumO! ^ (-.6)
Oo4! = f! * sumO2!

'OUTPUT TO A FILE ALTITUDE VERSES CN2 FOR EACH CHANNEL TO BE
'PLOTTED WITH SUPERCALC

INPUT "enter output file name ", output$
OPEN output$ FOR OUTPUT AS #3

FOR i = start TO stp
    WRITE #3, dta(i, 11), dta(i, 14), dta(i, 15), dta(i, 16),
        dta(i, 17)
NEXT i

PRINT
PRINT "Ro11= ", ro1!
PRINT "Ro2= ", ro2!
PRINT "Ro3= ", ro3!
PRINT "Ro4= ", ro4!
PRINT "Oo1= "; Oo1!
PRINT "Oo2= "; Oo2!
PRINT "Oo3= "; Oo3!
PRINT "Oo4= "; Oo4!

END

```

```

REM $STATIC
DEFSNG I-N
SUB Crout (a(), b(), c)
    DEFINT I-M
    ' this subroutine solves the set of simultaneous equations
    ' A*X=B where A is a symmetric matrix using the Crout or
    ' Cholesky procedure.
    ' The original A and B arrays are destroyed.
    m = c
    a11 = a(1, 1)
    IF a11 = 0 THEN GOTO singular
    FOR i = 2 TO m
        a(1, i) = a(i, 1) / a11
    NEXT i
    b(1) = b(1) / a11
    '

```

```

'set up auxiliary matrix
,
FOR j = 2 TO m
  j1 = j - 1
  FOR i = j TO m
    asave = 0!
    FOR k = 1 TO j1
      asave = asave + a(i, k) * a(k, j)
    NEXT k
    a(i, j) = a(i, j) - asave
    IF i > j THEN a(j, i) = a(i, j) / a(j, j)
  NEXT i
  bsav = 0!
  FOR k = 1 TO j1
    bsav = bsav + a(j, k) * b(k)
  NEXT k
  ajj = a(j, j)
  IF ajj = 0 THEN GOTO singular
  b(j) = (b(j) - bsav) / ajj
NEXT j
,
' back substitution and calculate determinant
,
m1 = m - 1
FOR i = 1 TO m1
  bsav = 0!
  mi = m - i
  mi1 = mi + 1
  FOR j = mi1 TO m
    bsav = bsav + a(mi, j) * b(j)
  NEXT j
  b(mi) = b(mi) - bsav
NEXT i
GOTO finished

singular:
  PRINT "***Matrix is singular***"
finished:
END SUB

DEFSNG I-M
FUNCTION temp (r, b())
  lnr = LOG(r)
  temp = 1! / (b(1) + lnr * (b(2) + lnr * (b(3) + b(4) * lnr)))
END FUNCTION

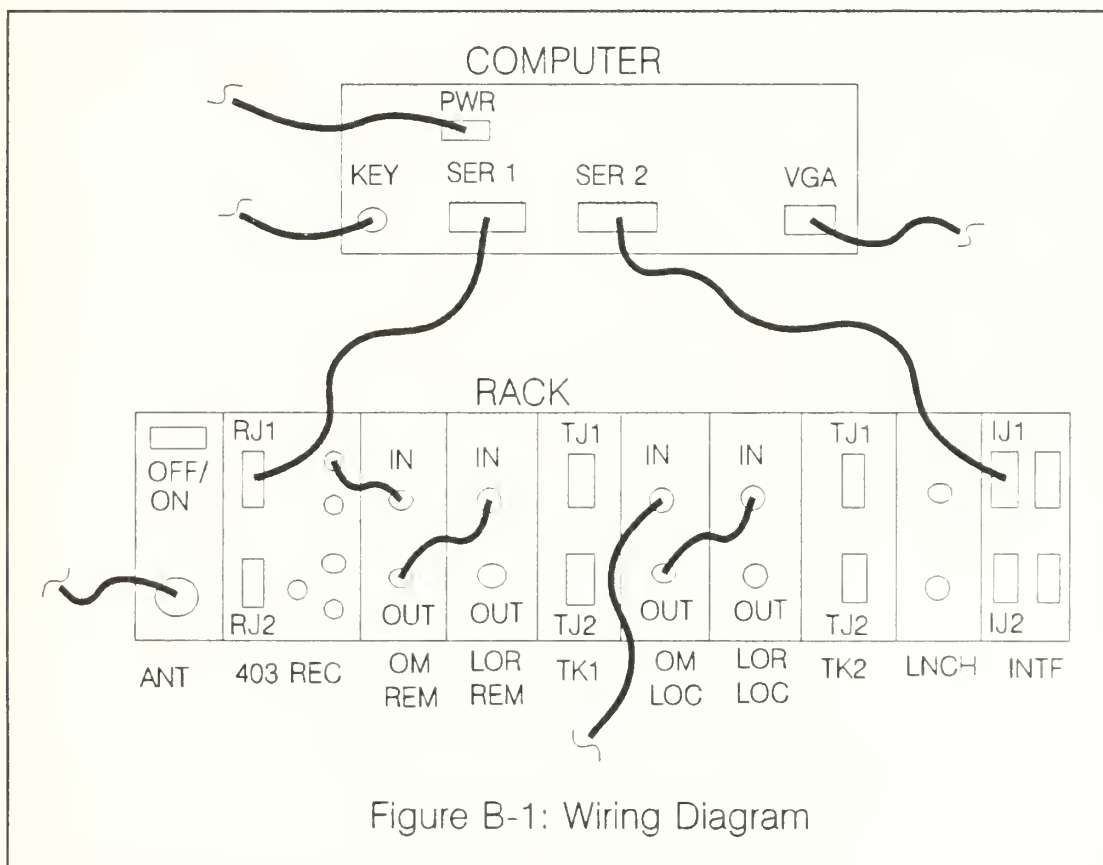
```

## APPENDIX B. NOTES ON OPERATION OF VIZ-9000 SYSTEM

The following are notes to support the operation of the VIZ system. They are to be used in conjunction with the manufacturer's manual. These notes are a brief summary of the steps the NPS group found to be important upon initial indoctrination of how to use the VIZ system.

### PART I

- The initial wiring of the system should be as shown in figure B-1.



## PART II

- After properly connecting all the cables, and properly installing the navigation and receiver antennas, the system should be booted up ensuring the "rack" is turned on before the computer.

(WARNING: be sure the nav antenna is not too close to the receiver antenna before starting the system. The receiver antenna makes a complete rotation upon energizing and can damage a nearby nav antenna.)

- The next step is to run "SETUP". SETUP consists of 8 parts. The following configuration should be used for the Monterey Bay area:

\*\*\*Whenever data is selected or entered, to leave the present screen and return to the previous menu, press "escape" and follow the directions on the screen.

1) Station Installation:

Customer Name: NPS  
Station ID: NPS  
LAT: 36° 35' 42.0 N  
LONG: 121° 52' 57.0 W  
WMO station no: 0  
Station Ht: 38 m (2500 m MAX)  
Local time: 0  
Surface data timer: 0  
Sonde type: 2  
PTU selection: Y

2) Receiver Installation:

start-stop: 395-410 hz

3) Navaid Installation:

Zeemet system: LORAN  
Tracker 1: LORAN  
Tracker 2: OMEGA

\*\*\*\*If desire an omega launch, then just toggle the zeemet system to omega (by using space bar), nothing else has to be changed.

\*\*\*\*For cross chain loran flight, change tracker 2 to loran.

After entering "LORAN, LORAN, OMEGA", go to tracker 1 and press "enter". This will open a sub-window to choose what loran chain you want. Highlight "9940" and press the space bar so the "check mark" moves to 9940. Next press "escape", go to tracker 2, press "enter", and now select for omega:

OMEGA  
Japan: include  
Norway: exclude  
Liberia: exclude  
Hawaii: include  
North Dakota: common  
La Reunion: include  
Argentina: include  
Australia: include

4) Wind Computation (done in height)

LORAN  
1. 0 60 2 15  
2. 1000 90 3 15  
3. 10000 120 4 15

OMEGA  
1. 0 120 4 15  
2. 1000 180 5 15  
3. 10000 240 7 15

5) Loran Chain File:  
-leave untouched

6) Antenna Configuration:

The cycle time needs to be rechecked at least yearly. Presently the cycle time is 48.3 sec.

\*\*\*\*Remember at the end of this menu to adjust antenna center for each site (need magnetic variation for site). For Monterey, magnetic variation is 16° East, therefore compass heading should read 074 (so yagi antenna points 090 T).



6) Antenna Configuration (continued):  
mode: auto  
select: omni  
systems: both  
switch: 4000 m down range

When this information is entered, antenna will cycle and stop at its midpoint.

This is when the orientation should be adjusted (adjust antenna to most probable wind azimuth).

### PART III

- To run a flight:

- 1) choose which type of sonde (loran or omega)
- 2) fill balloon and attach sonde
- 3) get permission from Monterey Airport tower to launch (375-1214)
- 4) type "START"

- When menu appears, enter sonde serial number and flight ID:

flight ID = month + day + hour (2 digits each)  
EX: 031121 = March 11, 2100

- Once this is entered, check Navaid status. Use instruments to enter surface data.

- Once sonde is prepared, check receiver status (signal strength should be 200-255). Receiver should lock on sonde after a few minutes. If not, go to receiver display [Alt-s] to observe sweep of spectrum.

- Next check calibration. Check to see that temperature and humidity lock-in numbers match those on sonde sticker (if close, go with computer, if way off, go with sonde label). Enter offsets if needed.

- Finally, when "?"'s" on 1-4 have changed to "\*"s", arm for launch. You can launch the sonde at anytime after you press arm for launch. However, do not hold the sonde too long because you only have two hours of allotted time from the "arm for launch" time for a complete flight.

- Wait a few minutes for PTU data to show up on the screen.

- Once you have PTU data, go to "Data Display Mode". Choose the PTU plot display.

- Check ascent rate for 180-240 m/min.

- At any time in the flight you can check on the pointing of the antenna and S/N ratio levels by going to "utilities".

\*\*\*\*Do not go to receiver mode in utilities once launch has started. This will cause a stopping of data collection.

- When flight has finished, you should be in either PTU plot or general flight menu screen. Now go to utilities to save flight data to disk.

- After this is done, you can exit flight menu.

## APPENDIX C. PLOTS OF $C_n^2$

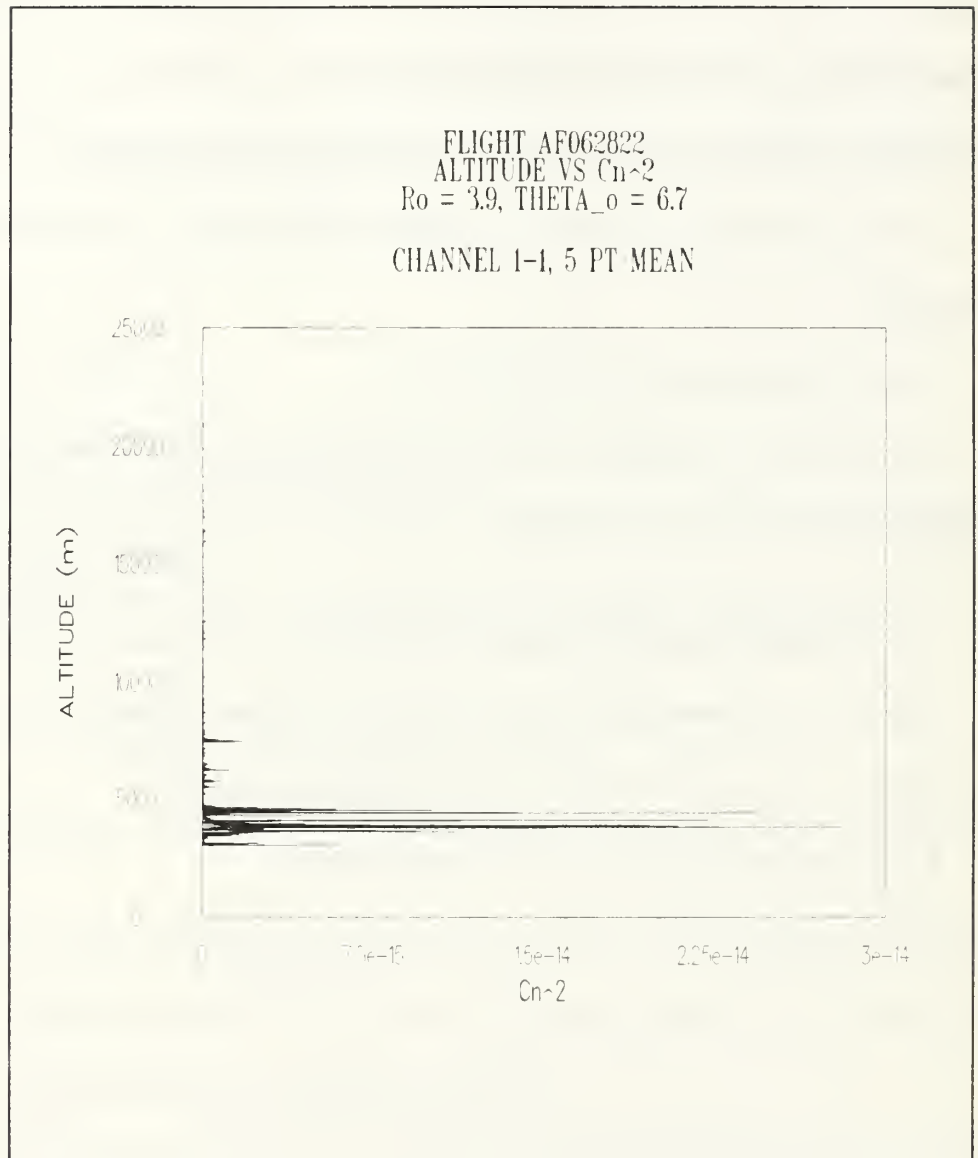


Figure C-1: Altitude verses  $C_n^2$

FLIGHT AF062922  
 ALTITUDE VS  $C_n^2$   
 $R_0 = 2.3$ ,  $\theta_0 = 11.3$

CHANNEL 1-1, 5 PT MEAN

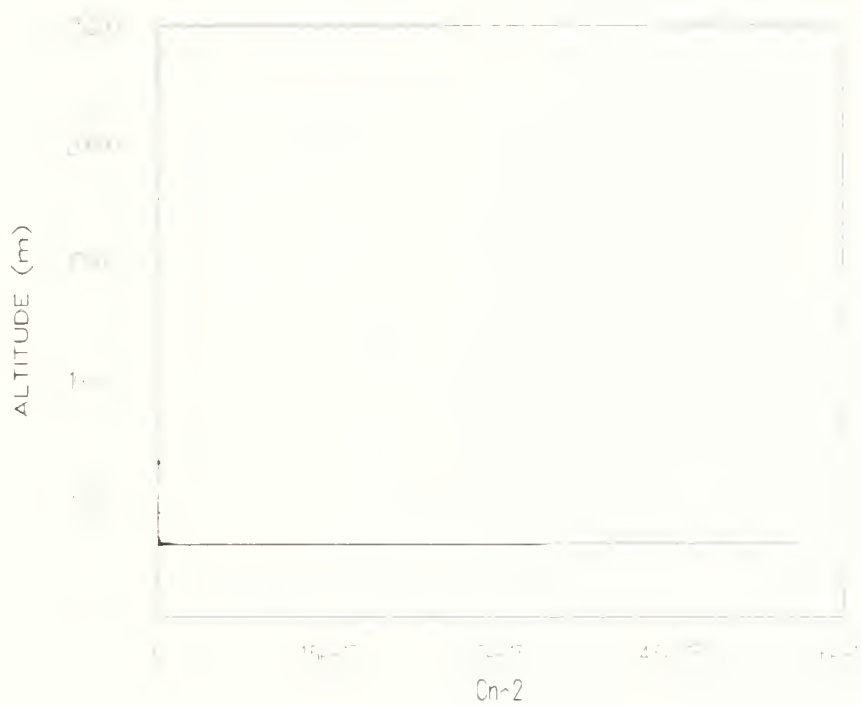


Figure C-2: Altitude verses  $C_n^2$

FLIGHT AF063021  
ALTITUDE VS  $C_n^2$   
 $R_0 = 8.9$ ,  $\text{THETA}_0 = 5.4$

CHANNEL 1-1, 5 PT MEAN

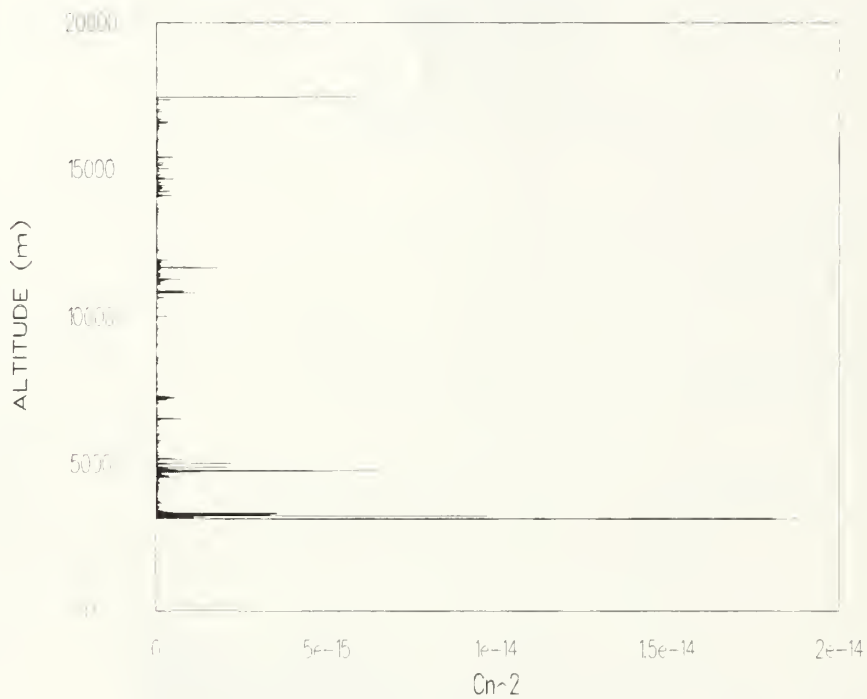


Figure C-3: Altitude verses  $C_n^2$

FLIGHT NS11522  
ALTITUDE VS  $C_n^2$   
 $R_0 = 4.9$ ,  $\text{THETA}_0 = 3.3$

CHANNEL 2-1, TWO POINT PROBE

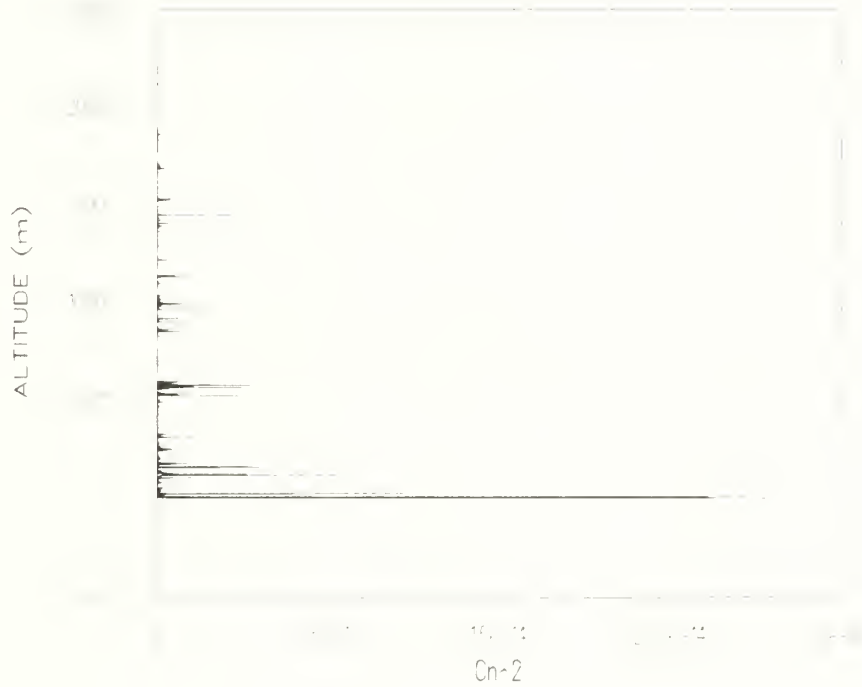


Figure C-4: Altitude verses  $C_n^2$



FLIGHT NS111522  
ALTITUDE VS  $C_n^2$   
 $R_0 = 3.5$ ,  $\text{THETA}_0 = 3.1$

CHANNEL 1-1, 5 PT MEAN

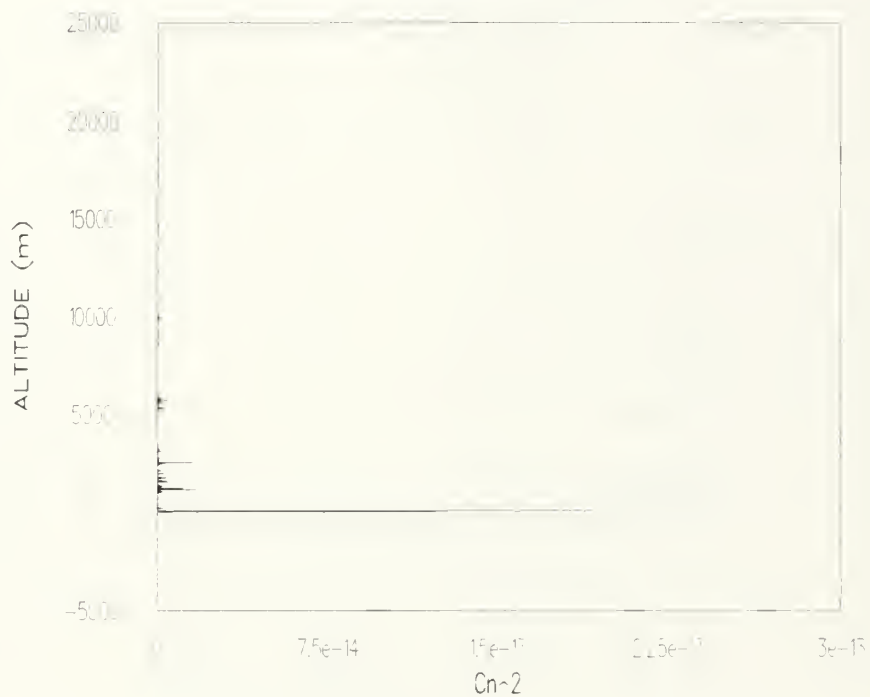


Figure C-5: Altitude verses  $C_n^2$

## APPENDIX D. PROBE HEATING

Figure D-1 is a plot showing the effect of probe heating from channel 1 to 4. As shown, the probe temperature increases from channel 1 to 2, then decreases on channel 4. This is because the probe is off between channels 2 and 4 (no data on channel 3) allowing the probe to cool.

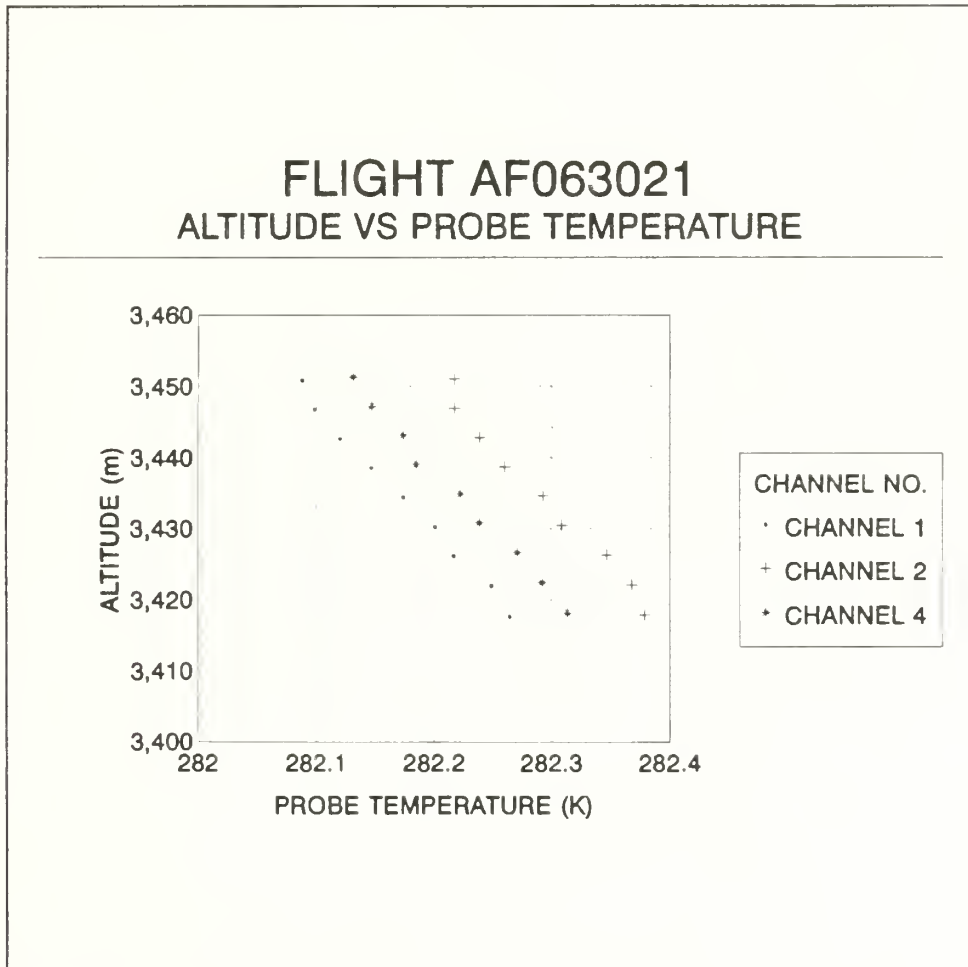


Figure D-1. Probe Heating

## APPENDIX E. EFFECTS OF CONVERTING COUNTS TO RESISTANCE

The VIZ Microsonde II measures resistance by counting clock pulses and then converting these counts into resistance values. In order to keep resolution high, the counts stay between  $2^{14}$  and  $2^{16}$ . When the counts fall below  $2^{14}$  the system doubles the number of periods counted (racheting effect). Figures E-1 through E-7 show the effects of these rachet points. The two times the system racheted were found to be at resistances of 60 and 260 k $\Omega$ .

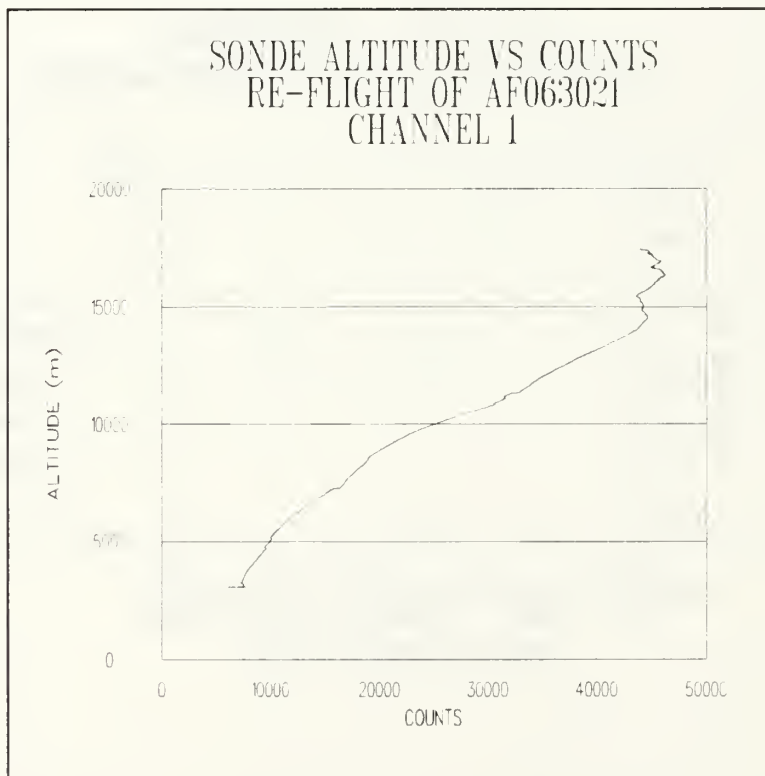


Figure E-1: Racheting Effect on Counts

SONDE ALTITUDE VS COUNTS  
RE-FLIGHT OF AF063021  
CHANNEL 1



Figure E-2: Racheting Effect on Counts

# SONDE ALTITUDE VS COUNTS RE-FLIGHT OF AF063021 CHANNEL 1

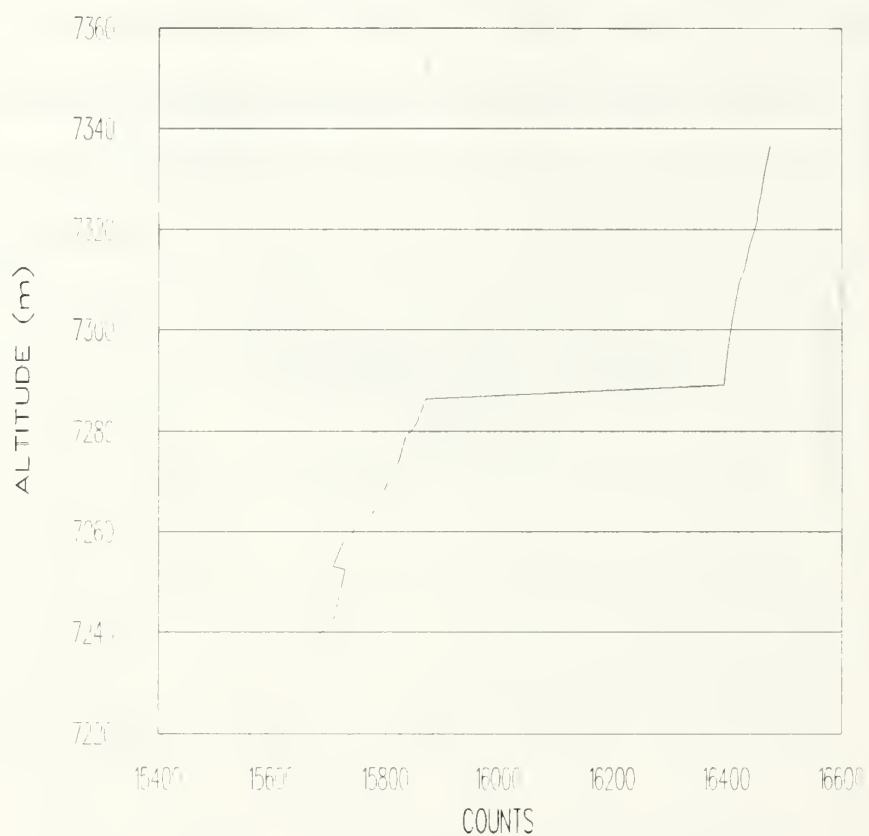


Figure E-3: Racheting Effect on Counts

SONDE ALTITUDE VS COUNTS  
RE-FLIGHT OF AF063021  
CHANNEL 4

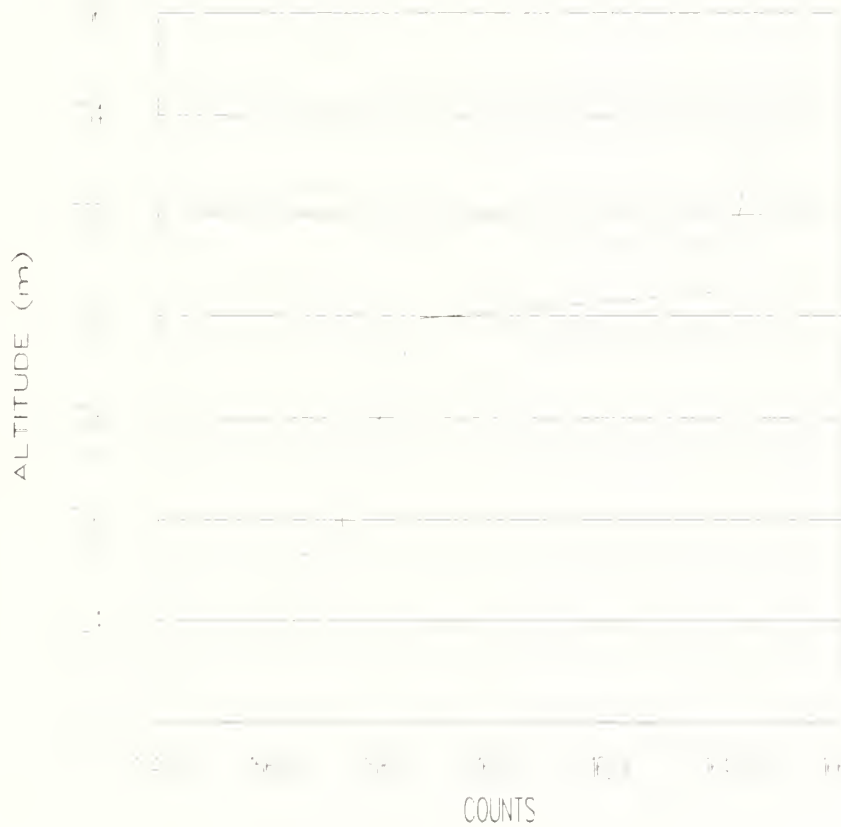


Figure E-4: Ratcheting Effect on Counts

FLIGHT AF063021  
ALTITUDE VS DELTA T  
CHANNEL 4-1

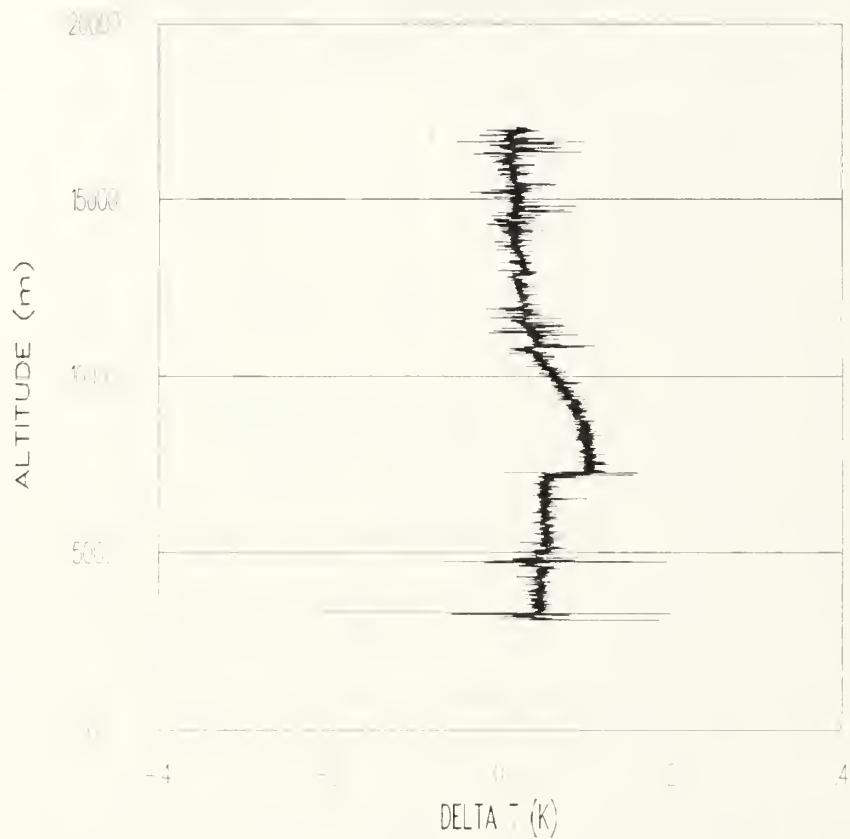


Figure E-5: Ratcheting Effect on Delta T



FLIGHT AF063021  
ALTITUDE VS DELTA T  
CHANNEL 4-1

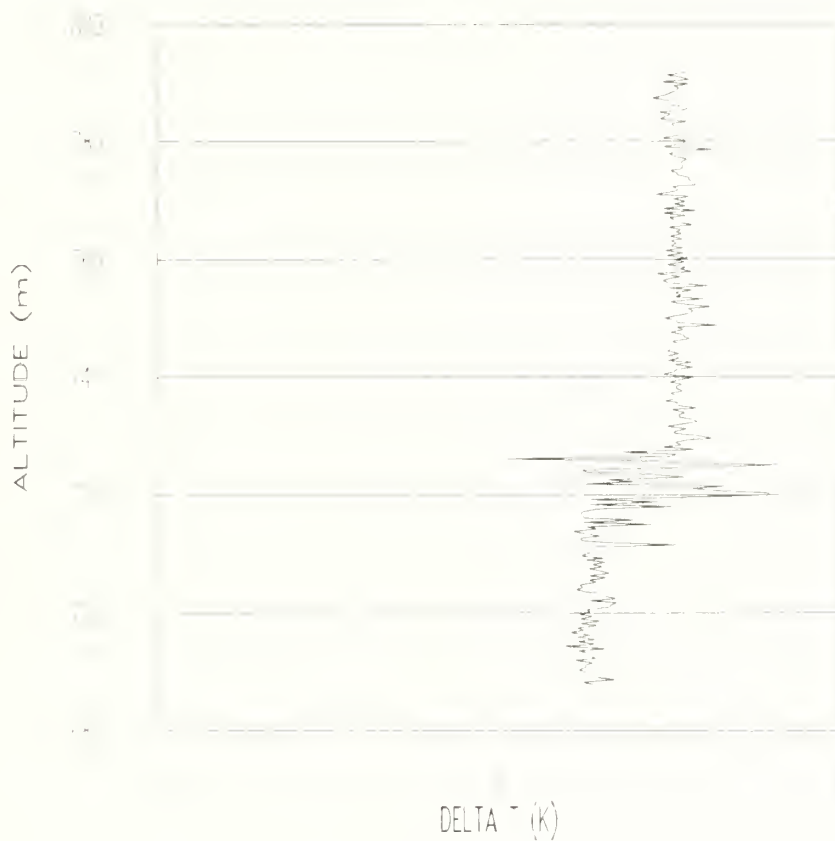


Figure E-6: Racheting Effect on Delta T

FLIGHT AF063021  
ALTITUDE VS (DELTA T -  $\Delta T$ )  
CHANNEL 4-1

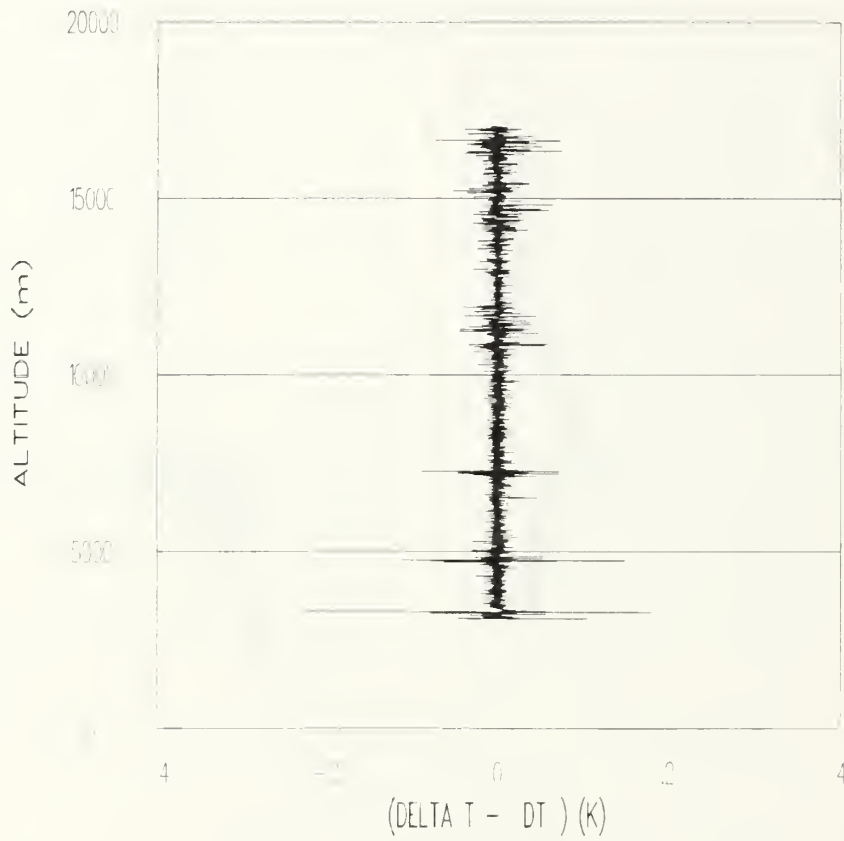


Figure E-7: Ratcheting Effect on Processed Data

## LIST OF REFERENCES

1. Gebhardt, F. G., "High Power Laser Propagation", Applied Optics, Vol. 15, No. 6, June 1976.
2. Tatarski, V.I., Wave Propagation in a Turbulent Medium, Dover Publications, Inc., New York, 1961.
3. Nelson, D., Atmospheric Turbulence Effects In the Relay Mirror Experiment, M.S. Thesis, Naval Postgraduate School, Monterey, California, June 1988.
4. Strohbehn, J.W., "Laser Beam Propagation in the Atmosphere", Topics In Applied Physics, Vol. 25, New York, 1978.
5. Suits, G.H., "Propagation Through Atmospheric Turbulence", The Infrared Handbook, Environmental Research Institute of Michigan, Ann Arbor, Michigan, 1985.
6. Walters, D.L. and Kunkel, K.E., "Atmospheric Modulation Transfer Function for Desert and Mountain Location: The Atmospheric Effects on  $r_o$ ", Journal of the Optical Society of America, Vol. 71, April 1981.
7. Fried, D.L., "Optical Resolution Through a Randomly Inhomogeneous Medium for Very Long and Very Short Exposures", Journal of the Optical Society of America, Vol. 56, August 1966.
8. Reviews of Modern Physics, Vol. 59, No. 3, Part 2, July 1987.
9. Fried, D.L., "Anisoplanatism in Adaptive Optics", Journal of the Optical Society of America, Vol 72. pp. 52-61, 1982.
10. Weitekamp, M.R., Investigation of the Source of Thermosonde Measured Diurnal Variation of Optical Turbulence, M.S. Thesis, Naval Postgraduate School, Monterey, California, December 1990.
11. Steinhart, J.S. and S.R. Hart, "Calibration Curves for Thermistors", Deep-Sea Research, Vol. 15, 1968.

12. Kiefer, D.A., Development of a Single Point Temperature Probe to Measure the Temperature Structure Parameter, M.S. Thesis, Naval Postgraduate School, Monterey, California, June 1990.
13. Mattingly, T.S., Measurement of Surface Layer Optical Turbulence Above AMOS, M.S. Thesis, Naval Postgraduate School, Monterey, California, December, 1991.
14. Hecht, E. and Zajac, A., Optics, Addison-Wesley, Menlo Park, California, 1988.
15. Lutomirski, R.F. and Yura, H.T., "Wave Structure Function and Mutual Coherence Function of an Optical Wave in a Turbulent Atmosphere", Journal of the Optical Society of America, Vol. 61, No. 4, April 1971.

## INITIAL DISTRIBUTION LIST

	No. Copies
1. Defense Technical Information Center Cameron Station Alexandria, VA 22304-6154	2
2. Library, Code 52 Naval Postgraduate School Monterey, CA 93943-5002	2
3. Professor Karlheinz E. Woehler Chairman, Department of Physics Naval Postgraduate School (Code PHWh) Monterey, CA 93943	1
4. Professor Donald L. Walters Naval Postgraduate School (Code PHWe) Monterey, CA 93943	5
5. Capt Ann Slavin PL/LTE Phillips Laboratory Kirtland Air Force Base New Mexico 87117	1
6. Andrew Terzakis PL/WE Phillips Laboratory Kirtland Air Force Base New Mexico 87117	1









DUDLEY H. MOORE LIBRARY  
NAVAL POSTGRADUATE SCHOOL  
MONTEREY, CALIF. 94064-5101

Richardson,  
ID: 327680r  
H737  
Investi-  
\Hoove-  
due: 6

GAYLORD S





DUDLEY KNOX LIBRARY



3 2768 00019256 1